Coplanar Strip Line based Technique for the measurement of Defects in GFRP wrapped Concrete Structures

A Thesis
submitted towards the partial fulfilment of requirement
for the award of degree of

Master of Engineering
In
Electronics and Communication

Submitted by
Devinder Sharma
Roll no:-800961005(ECED)

Under the guidance of
Dr. Abhijit Mukherjee
Director, Thapar University

Dr. Rajesh Khanna
Professor (ECED)

Dr. Shweta Goyal
Assistant Professor (CED)

DEPARTMENT OF ELECTRONICS AND COMMUNICATION ENGINEERING
THAPAR UNIVERSITY
PATIALA-147004 (PUNJAB)

JULY-2011

CERTIFICATE

I, Devinder Sharma hereby certify that the thesis report entitled **"Coplanar Strip Line based technique for the measurement of Defects in GFRP wrapped Concrete Structures"** is an authentic record of my study carried out as requirement for the award of degree M.E. (Electronics and Communication) at Thapar University, Patiala under the guidance of Dr. Abhijit Mukherjee, Dr. Rajesh Khanna and Dr. Shweta Goyal and referred other researcher's work which are duly listed in the reference section.

The matter present in this thesis has not been submitted in any University/ Institution for the award of Master of Engineering.

Devinder Sharma
Roll no. 800961005

This is certified that the above statement made by the student is correct to the best of my knowledge and belief.

(Dr. Abhijit Mukherjee)
Director
Thapar University, Patiala

(Dr. Rajesh Khanna)
Professor, ECED
Thapar University, Patiala

(Dr. Shweta Goyal)
Assistant Professor, CED
Thapar University, Patiala

Professor & H.O.D, ECED
Thapar University, Patiala

(Dr. S. K. Mohapatra)
Dean (Academic Affairs)
Thapar University, Patiala

ACKNOWLEDGEMENT

I would like to give special thanks to my guide **Dr. Abhijit Mukherjee**, Director, Thapar University, Patiala, for his advice, kind assistance, and invaluable guidance. It has been a great honour to work under him.

I would like to express my deepest gratitude to my guide **Dr. Rajesh Khanna**, Professor, Electronics and Communication Engineering Department, Thapar University, Patiala, for his advice, motivation, guidance, moral support, efforts and the attitude with which he solved all of my queries in making this thesis report possible. It has been a great honour to work under him.

I am also thankful to **Dr. A.K. Chatterjee**, Professor&Head, Electronics and Communication Engineering Department for providing us with adequate infrastructure in carrying the work.

The thanks are also due to my guide **Dr. Shweta Goyal**, Assistant Professor, Civil Engineering Department, for her advices and support which help me for my work.

I am also thankful to **Dr. Rahul Chhibber**, Assistant Professor, Mechanical Engineering Department, for his advice and support in my work.

I would also like to thank all the faculty members of ECED and CED for their intellectual support and also special thanks to my family and my friends who constantly encouraged me to complete this work. I am also thankful to the authors whose work I have consulted and quoted in this work.

Devinder Sharma

(800961005)

ABSTRACT

The introduction of FRP (Fiber Reinforced Polymer) composites in civil engineering applications has resulted from the need for structural rehabilitation of aging infrastructure such as bridges, roads, buildings etc. The structural integrity of FRP bonded systems is dependent on proper bonding between the FRP wrap and the underlying members. The bond integrity may be adversely affected when air and water voids occurs. Therefore, it is important to evaluate the FRP retrofitted structural members using non destructive evaluation techniques such as infrared thermo graphic, ultrasonic, microwave method, acoustic, radiographic technique and capacitive sensor based technique. An NDT (Non Destructive Testing) method would not only locate a defect, but it would also be useful for determining characteristics of the defect such as its size, shape, and orientation. Many NDT techniques have the ability to detect and characterize defects in structures made entirely of composite materials and also structures rehabilitated with FRP wraps. All above mentioned NDT techniques has some advantages as well as disadvantages.

This thesis presents a new non destructive evolution technique for measuring the defects and delamination in Glass Fiber Reinforced Polymer (GFRP) wrapped CONCRETE using coplanar strip lines. CPS based technique is cost effective and locate the defects very easily. If there is presence of air and water void in the GFRP and CONCRETE then the change in the capacitance & electric field of CPS at low frequency and change in the reflection coefficient and resonant frequency at radio frequency (RF) takes place. As the width of air or water void increases the change in capacitance of CPS (Coplanar Strip Line) at low frequency can be measured. That's why CPS based method is most suitable to measure the capacitance. To find the capacitance due to air or water void in FRP and concrete different models are made using Maxwell 2D software at low frequency. At high frequency, the alternation in the resonant frequency due to addition of moisture on CST Microwave studio 9.0 is studied.

Keywords: GFRP, NDT, FRP, FEM, Composites, Air void, Water void, Capacitance, Coplanar strip lines, Reflection coefficient, Capacitive imaging.

TABLE OF CONTENTS

LIST OF FIGURES

Figure no. **Page no.**

LIST OF TABLES

Table no. **Page no.**

LIST OF ABBREVIATIONS

C	Capacitance (F);
C_s	Partial capacitance due to substrate;
CPS	Coplanar strip line;
ε_{eff}	Effective dielectric permittivity for the substrate layers;
ε_o	Permittivity of free space F/m;
ε_r	Dielectric permittivity of the material;
g	Electrode spacing mm;
G	Conductance per unit length of a CPS;
L	Inductance per unit length of a CPS;
M	Moisture absorption ratio;
h	Height of the substrate layer mm;
K(k)	Elliptic integral of first kind;
r	Resistance per unit length of a CPS;
s	Electrode width mm;
k	Modulus of the of complete elliptic integral for first kind function;
l	Electrode length mm;
WV	Woven fiber;
Z	Impedance of a single layer;
FRP	Fiber Reinforced Polymer;
NDT	Non Destructive Techniques;
CPS	Coplanar Strip Line;

GFRP	Glass fiber reinforced polymer;
RC	Reinforced concrete
MSPA	Micro strip patch antenna

Chapter 1

Introduction

1.1 Introduction

Non destructive testing (**NDT**) is a wide group of analysis techniques used in science and industry to evaluate the properties of a material, component or system without causing damage. Because NDT does not permanently alter the article being inspected, it is a highly-valuable technique that can save both money and time in product evaluation, troubleshooting and research. [1]

Non-Destructive Testing (N.D.T.) is one part of the function of Quality Control and is complementary to other long established methods.By definition non-destructive testing is the testing of materials, for surface or internal flaws or metallurgical condition without interfering in any way with the integrity of the material or its suitability for service.

1.1.1 When and Where we use NDT Techniques

WHEN?

These are the subsequent areas in which NDT techniques are used:-

- To assist in product development
- To screen or sort incoming materials
- To monitor, improve or control manufacturing processes
- To verify proper processing such as heat treating
- To verify proper assembly
- To inspect for in-service damage

WHERE?

These are the subsequent fields in which NDT techniques are found:-

- Storage tank inspection
- Power plant inspection
- Rail inspection
- Aircraft inspection
- Bridge inspection

In figure 1.1 to 1.5, shows the different areas where NDT techniques is used to inspection:-

Figure 1.1 Storage tank inspection [1]

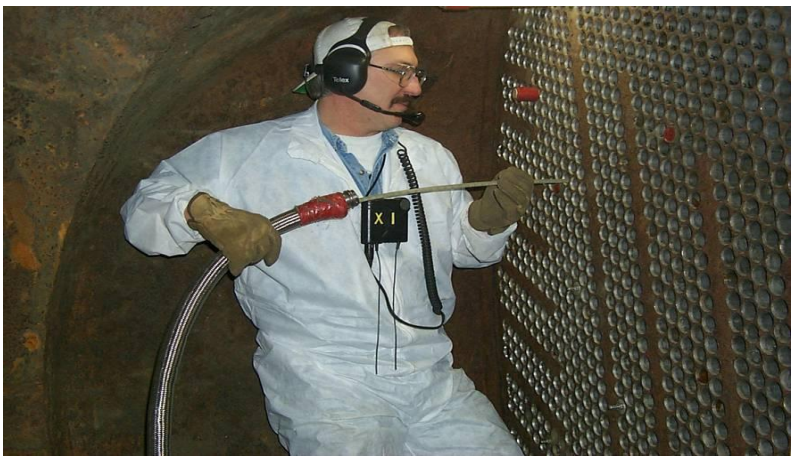

Figure 1.2 Power plant inspection [1]

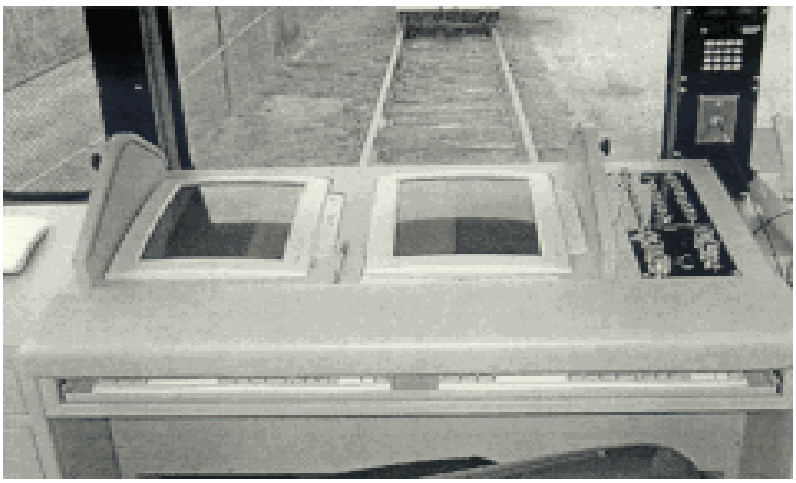

Figure 1.3 Rail inspection [1]

Figure 1.4 Aircraft inspection [1]

Figure 1.5 Bridge inspection [1]

1.2 Use of NDT in Reinforced Concrete Structures

Reinforced concrete is concrete in which reinforcement bars ("rebars"), reinforcement grids, plates or fibers have been incorporated to strengthen the concrete in tension. Reinforced Concrete structures have the potential to be very durable and capable of withstanding a variety of adverse environmental conditions. However, failures in the RC structures do still occur due to adverse effects of external or environmental agencies such as weathering, attack by natural or industrial chemicals and gases etc. causing the loss in service life. Certain internal agencies are also responsible for causing damage to the structures such as harmful alkalis, aggregate reactions, presence of sulphates and chlorides from the ingredients of concrete. Ingress of moisture or air through the cracks developed may lead to the corrosion of reinforcement. The resulting corrosion products occupy volumes larger than that of the steel. The increased volume induces tensile stresses in the concrete leading to

further cracking and spalling of concrete cover. As a result, the reinforcements get exposed to direct environmental attack and the corrosion is accelerated. Corrosion also reduces the cross section of reinforcement and there by the load carrying capacity of the structure. In general, corrosion weakens the structure to a high degree hence for the safety and reliability of RC structure, it is necessary to consider the assessment of cracks in concrete and monitoring of corrosion in reinforcement embedded in concrete. Therefore for the assessment of cracks we use the NDT techniques.

1.3 Use of NDT in Retrofitted Structures

In general, corrosion weakens the structure to a high degree, hence, for the safety and reliability, it is necessary to rehabilitate and repair of RC structure even after repair of the structure and to monitor the condition of structure we use the NDT techniques.

Fiber Reinforced Polymer (FRP) composites have an extensive history of successful use in the aerospace, defence, marine, corrosion resistant equipments and automotive sectors. However until few years back they were largely considered to be of limited value in civil infrastructure beyond use in facades, aesthetic additions and for architectural purposes. But now there has been growing interest in the use of composites due to advances in low cost manufacturing methods, reduced material demand in high cost areas (for example defence) the ability to mould complex shapes, and the economic viability of composites when combined with conventional materials.

FRP composites today are used in variety of applications ranging from replacement for steel rebar's and tendons used conventionally as tensile reinforcement in concrete, jackets for retrofitting of column and externally bonded reinforcement for the rehabilitation of deteriorating structural systems, to use in all composite structures such as building frames and even bridge decks. Despite their relative newness, these materials (primarily using E glass and carbon reinforcing fibers), are being increasingly adopted for specific applications on part with, and even in preference to conventional materials such as steel and concrete. The attractiveness of composites is not merely based on performance attributes such as high specific strength and specific stiffness and corrosion resistance, but also due to their light weight and ease of

installation in the field, ability for rapid installation and potential for long term durability.

Composites have found their maximum current use as material for rapid and cost effective rehabilitation (retrofit, repair and strengthening) of deteriorated and under-strength structural concrete components. New construction with composites has also become of interest in the civil and the structural engineering areas.

However like other materials, FRP can have defects and can decay during the service life. Defects in composites may be due to several factors including improper design, fabrication and manufacturing. During manufacturing of FRP's due to poor workmanship some defects may occur between interface of FRP and concrete. This may adversely affect the fiber matrix adhesion properties, resulting in debonding at the fiber/matrix interfaces, micro-cracking in the matrix, fiber fragmentation, continuous cracks and several other phenomena that may actually degrade the mechanical properties of the composites. So, assessment of cracks in FRP and monitoring of delamination of FRP is also required. For this purpose, NDT techniques are used.

1.4 NDT Techniques to Detect the Defects

The structural performance of FRP bonded system is dependent on proper bonding between the FRP wrap and the underlying members. The bond integrity may be adversely affected when damage occurs. Therefore, it is important to evaluate the FRP retrofitted structural members using non destructive evaluation techniques such as infrared thermography, ultrasonics, microwave methods, acoustic, capacitive sensor based technique and radiographic methods. An NDE method would not only locate a defect such as its size, shape and orientation. A number of NDT techniques are available for assessing internal features such as voids, fiber volume fraction, fiber wash, interlaminar and translaminar cracks, lay up orders etc. in FRP composites. The various non destructive evolution techniques are categorized into radiography, microwave, thermography, ultrasonic, acoustic emission and capacitive sensor based technique etc.

Radiography (RT) Radiography involves the use of penetrating gamma or X ray radiation to examine parts and products for imperfections. An X-ray generator or

radioactive isotope is used as a source of radiation. The resulting shadowgraph shows the dimensional features of the part. Possible imperfections are indicated as density changes on the film in the same manner as medical X-ray shows broken bones.

Microwave (MW) It is an electromagnetic (EM) imaging technology for detecting voids and debonding between the jacket and the column, which may significantly weaken the structural performance of the column otherwise attainable by jacketing. This technology is based on the reflection analysis of a continuous EM wave sent toward and reflected from layered FRP adhesive-concrete medium: Poor bonding conditions including voids and debonding will generate air gaps which produce additional reflections of the EM wave.

Thermographic (TP) In this technique such as infrared thermographic, pulsed infrared thermographic inspection, lock-in thermographic etc are based on the temperature disorder that appears in the material to be tested due to the thermal insulation provided by the defect. The thermographic techniques have been effective for identifying delaminations and offer potential for rapid inspection of concrete civil engineering structures that have been reinforced or rehabilitated with composite materials.

Ultrasonic Method (UT) is a non destructive testing method utilizing high-frequency sound waves to perform thickness measurements, corrosion checks, and internal discontinuity scans in welds, forgings, castings, and state-of-the-art composite materials. Defects or weak areas, such as flaws or wall thinning, are found by observing reflected sound energy (pulse echo testing) or by measuring energy lost as the ultrasonic sound waves travel through the material (transmission testing) under examination.

Acoustic Emission (AE) is the class of phenomena where an elastic wave originating from subsurface cracks propagate through the solid to the surface, where it can be recorded by one or more sensors. The AE sensor is a receiving transducer that converts the mechanical wave into an electrical signal. In this way information about the existence and location of possible sources is obtained.

Capacitive sensor based method (CS) The proposed technique relies on detecting the variation of dielectric signatures in material compositions of the composite parts. The change in dielectric permittivity's as a result of damage, inside the composite material would produce a change in the measured capacitance and electric field at low frequency. At high frequency, micro-strip patch antenna is used to detect the defects in concrete, with the change in dielectric constant of the defect or void, resonant frequency changes and return loss also changes.

1.5 Why Coplanar Stripline method?

Above mentioned NDT methods indicated several difficulties associated with their field application due to the requirement for couplant, heat or wave source and sophisticated data analyzers with the limitations with respect to the coverage areas, detectable damage depth and the complications associated with data interpretation and portability. The main objective to use a coplanar strip line (CPS) method in detecting voids and delaminations is that we can use this method on a single plane, without the use of any conventional sandwich method or embedding a sensor in the structural itself. This technique provides a fast, effective, accurate, inexpensive and easy to implement method to measure the air and water voids in GFRP. This technique does not require any sophisticated data analyzer and can be easily used in field. We can use this method for the low and high frequency.

1.6 Objective of the Thesis

- Experimental and Simulation study of delamination in fiber-epoxy-fiber sheets.
- Experimental and Simulation study of capacitance with air and water void in GFRP wrapped concrete structures.
- Simulation study of variation of resonant frequency and reflection coefficient of concrete samples at high frequency with air and water void and steel rebar.

1.7 Organisation of the Thesis

After introduction of thesis in Chapter 1, Chapter 2 gives a brief description of FRP composites. This chapter also includes types of FRP composites, characteristics of polymer, fiber types, and uses of FRP for structural engineering applications.

Chapter 3 presents an extensive literature review on NDT techniques for the measurement of defects in GFRP based concrete structures which include Microwave, Coplanar capacitance measurements to evaluate the defects in FRP retrofits.

Chapter 4 deals with experimental and simulated measurement of capacitance of GFRP based CPS samples and concrete samples. The analytical expressions for capacitance per unit length of CPS using conformal mapping technique have been derived. In this chapter the technique of sample preparation and experimental setup used are described in detail.

Chapter 5 deals with the simulated results at high frequency using micro strip patch antenna in terms of resonant frequency and reflection coefficient with the moisture ingress on the substrate and with the presence of defects in GFRP wrapped concrete structures.

Chapter 6 finally gives the conclusion drawn from the work done in this thesis and the future scope for further research.

Chapter 2

Basics of FRP Composites

2.1 Composites

Composite materials consist of two or more materials combined in such a way that the individual materials are easily distinguishable. The individual materials that make up a composite are called constituents. Most composites have two constituent materials: a binder or matrix, and reinforcement. The reinforcement is usually much stronger and stiffer than the matrix, and gives the composite its good properties. The matrix holds the reinforcements in an orderly pattern and also helps to transfer load among the reinforcements. The most common composites are those made with strong fibers held together in a binder. Composites that use more than one type of reinforcement material are called hybrids. When the same properties are desired in every direction on the plane of the lamina, randomly oriented fibers are used. Composite materials are available as plies or lamina. A single ply consists of fibers oriented in a single direction (unidirectional) or in two directions (bidirectional; for example a woven fabric). Composite properties are best in the direction of the fibers. In the direction perpendicular, or transverse, to the fibers, the matrix properties dominate because load must be transferred by the matrix every fiber diameter. Because most structures are not loaded in a single direction, even though one direction may dominate, it is necessary to orient fibers in multiple directions. This is accomplished by stacking multiple plies together. Such a stack is called a laminate. [2]

Composite materials obtained by reinforcing polymer matrices using fibrous materials like glass, carbon or aramid are known as fiber reinforced polymers (FRP) or Advanced Composite Materials. The reinforcing fibers provides the composite with its structural properties such as high modulus of elasticity and high ultimate strength; whereas the matrix binds the fibers together, protects them from damage and distributes stresses among them. The fillers and additives are used as processor performance aids to impart special properties to the end product.

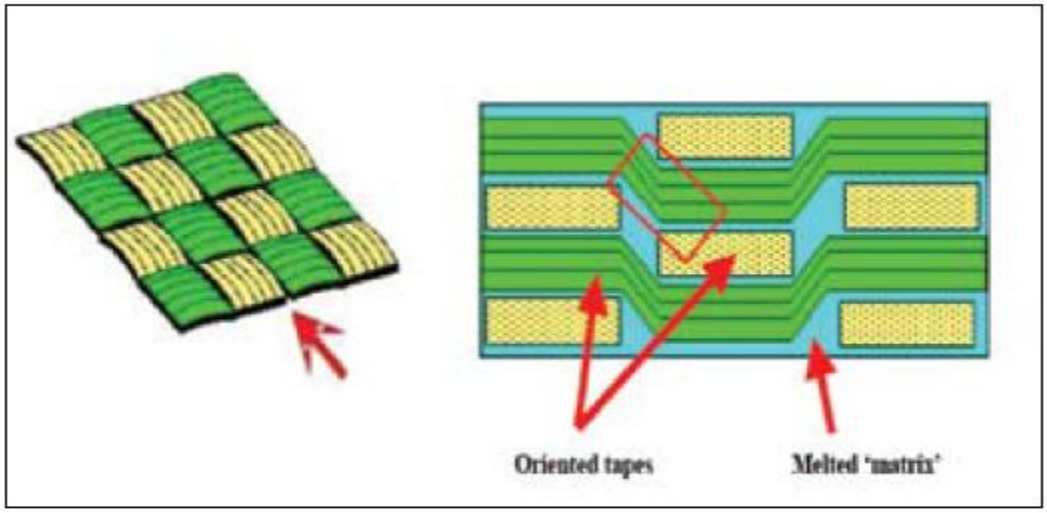

Figure 2.1: Schematic of the Composite formation [2]

2.1.1 Comparison between Composites and Metal

The basic difference of composite materials with metals is that they have an-Isotropic behaviour, which means that the properties of the composite material or formed laminate are directional depended. Metals have in general, an-Isotropic behaviour which means that the properties are same in all directions. Some other differences are: [2]

- End material is formed during production process, in most cases in the end form of the end product.
- Materials habits are also determined by production/curing process
- Fibrous composites are more versatile than metals and can be tailored to meet performance needs and complex design requirements.
- Higher specific strength (material strength/density material). Aramid and Carbon Fibre reinforced epoxies have approx. 4 to 6 times higher spec. tensile strength than steel or aluminium
- Great fatigue endurance especially for aramid and carbon reinforced epoxies, compared with metal.

2.2 Constituents of Composites

The two constituents of composites are polymers and resin. The following section discuss about both polymers and resin.

2.2.1 General Characteristics of polymers

Polymers are large molecules consisting of repeated chemical units (`mers') joined together. The “mer” or the repeated chemical units usually made of carbon, hydrogen, oxygen and/or silicon. To make the chain, many links or "-mers" are hooked or polymerized together. The units are called monomers, two of the units bonded together called as dimer, bonding of three units are called trimer and so on the bonding of many units leads to a polymer.

The chemical reaction in which the molecules of a monomer link together to form a polymer called a polymerization. Polymers may also be formed by poly condensation (addition polymer). When two or more monomers are involved, the product is called a copolymer. The transition period from a liquid state to a solid state during which an assembly is subjected to heat or pressure, or both, to cure the resin is called the curing time. After curing the product obtained will be in a solid state.

Polymers are typically classified into two categories depending upon the reaction to heating and cooling. They are called thermosets and thermoplastics. The important difference between these two categories is their behaviour under pressure and heat. Thermoset polymers are hygrothermally sensitive and can degrade at moderately high temperatures around 1600ºto 1800ºC in the presence of water whereas thermoplastic polymer is one which melts or flows when heated, and then capable of being shaped or reshaped while in its heated semi fluid state. Because of their unique properties thermoset and thermoplastic polymers are used for specific structural and non-structural applications. For example, thermosets are conventionally used for producing structural shapes whereas thermoplastics are typically used in many non-structural applications such as automobile panels, dashboards, door frames and so on.

2.2.2 Thermoplastic Polymers

A thermoplastic polymer is one which melts or flows when heated, and then capable of being shaped or reshaped while in its heated semi fluid state. Thermoplastic polymers are usually not highly cross linked, and act much like molecular solids: low melting and boiling points, low strength, ductile and the like. They occur in granular forms. Most thermoplastics are high molecular weight polymers whose chains associate through weak Vander Waals forces (polyethylene); stronger dipole-dipole

interactions and hydrogen bonding (nylon); or even stacking of aromatic rings (polystyrene). Thermoplastics do not require refrigerated storage, and they have virtually unlimited shelf and curing time. Also thermoplastic composites can be repaired because transition to the softened stage can be accomplished any number of times by application of heat.

2.2.3 Thermosetting Polymers (Thermosets)

Thermosets are usually malleable prior to curing, and designed to be moulded into their final form, or used as adhesives. In general, Thermoset polymers are called as resin system during processing and matrix after the curing. Thermoset resins have low viscosity, which allows for excellent impregnation of the fiber reinforcement and high processing speeds.

The curing process transforms the resin into a plastic or rubber by a cross-linking process. Energy and/or catalysts are added that cause the molecular chains to react at chemically active sites (unsaturated or epoxy sites, for example), linking into a rigid, 3-D structure. The cross-linking process forms a molecule with a larger molecular weight, resulting in a material with a higher melting point. During the reaction, when the molecular weight increases to a point so that the melting point is higher than the surrounding ambient temperature, the material forms into a solid material. Subsequent uncontrolled reheating of the material results in reaching the decomposition temperature before melting point. A thermoset material cannot be melted and re-shaped after it is cured.

Thermoset materials are generally stronger than thermoplastic materials due to this 3-D network of bonds, and are also better suited to high-temperature applications up to the decomposition temperature of the material.

2.3 Fiber Reinforced Polymer

Fiberglass reinforced plastic, commonly known as fiberglass, was developed commercially after World War II. Since that time, the use of fiberglass has grown rapidly. The term “fiberglass” describes a thermoset plastic resin that is reinforced with glass fibers

.

2.3.1 Properties of FRP Composites

The most common FRPs in civil engineering applications are glass fiber reinforced polymer (GFRP), carbon fiber reinforced polymer (CFRP) and aramid fiber reinforced polymer (AFRP). The fiber and matrices are combined in such a manner that the resulting composite material shows properties that are superior to those of its individual constituents. These properties mainly depend on the fiber volume, fiber orientation, mechanical properties of the constituents and the procedure used to fabricate the composite. FRP composites are anisotropic (properties vary with the direction). [3]

The functional requirements of fibers in FRP are as follows:

- They should have high modulus of elasticity to give stiffness to the composite.
- They should have high ultimate strength.
- They should have low variation of strength between the individual fibers.
- They should have stability during handling.
- They should have a uniform diameter.

A summary of typical Fiber properties is presented in Table 2.1[3]

The matrix should fulfil certain functions. These are:

- To bind the fibers together and to protect their surface from damage during the service life of the composite.
- To transfer stresses to the fibers efficiently by adhesion.
- To disperse the fibers and to separate them.
- To be chemically and thermally compatible with the fibers.

Table 2.1 Typical Fibre properties

Material	Density	Modulus of elasticity E	Strength in tension f_t	Strain in tension ε_t
	Kg/m^3	MPa	MPa	%
E-glass	2500	70000	1500-2500	1.8-3.0
S-glass	2500	86000	4800	-
High-Modulus Carbon	1950	380000	2000	0.5
High-Strength Carbon	1720	240000	2800	1.0
Carbon	1400	190000	1700	-
Boron	2570	400000	3400	-
Graphite	1400	250000	1700	-
Kevlar 49	1450	120000	2700-3500	2.0-2.7
Kevlar	1450	60000-130000	2900	-

A summary of typical Matrix properties is presented in Table 2.2 [3]

Table 2.2 Typical Matrix properties

Material	Density	Modulus of elasticity in tension E_t	Strength in tension f_t	Strength in compression f_c	Possion's ratio v	Co-efficient of thermal expansion α
	Kg/m^3	MPa	MPa	MPa		$10^{-6}/^oC$
Polyester	1200-1400	2500-4000	45-90	100-250	0.37-0.40	100-120
Epoxy	1100-1350	3000-5500	40-100	100-250	0.38-0.40	45-65
P.V.C	1400	2800	58	-	-	50
Nylon	1140	2800	70	-	-	100
Polyethylene	960	1200	32	-	-	120

A summary of typical Mechanical properties of GFRP are given in table 2.3 [3]

Table 2.3 Typical Mechanical properties of GFRP

Material	Fibre content	Density	Elasticity in tension E_t	Strength in tension f_t
	% by weight	kg/m^3	MPa	MPa
Unidirectional GFRP/Polyester laminate	50-80	1600-2000	20000-50000	400-1250
GFRP/Polyester Randomly Oriented Hand lay-up	25-25	1400-1600	6000-11000	60-180
GFRP/Polyester Material Metal Dye	25-50	1400-1600	6000-12000	60-200
GFRP/Polyester Woven Roving Hand Lay-ups	45-62	1500-1800	1200-2400	300-350
Sheet Moulding Compound Unidirectional Laminate	20-25	1750-1900	9000-13000	60-100
Carbon/Epoxy	70	1930	120000	800
Aramid/Epoxy	50-80	-	70000-80000	1000-1400

2.3.2 Advantages of Composites

The main features of the composite materials are their high fracture energy, ease of fabrication, and chemical inertness. The low cost is particularly true for glass reinforced polymers, which involve low material cost, compared to metal processing. The advantages of the composites over the conventional bulk materials are as follows:-

1. They can be made with high strength and high specific strength (ratio of strength to specific weight)
2. They can be made with high stiffness and high specific stiffness (ratio of stiffness to specific weight)
3. Their density is generally lower than other conventional construction materials.
4. Their strength can be high at elevated temperature.
5. Their impact and thermal shock resistance are good.

6. Their fatigue strength is good often better then metals.
7. Their oxidation and corrosion resistance are particularly good.
8. Their thermal expansion is low and can be controlled.
9. Their stress rupture life is better relative to many metals.
10. Their predetermined properties can be produced to meet individual needs.

FRPs are most commonly found as laminates, which are manufactured by unifying a number of thin layers of fibers and matrix into a desired thickness. Orientation and amount of fibers affect the properties of the laminates. Laminates may be available in unidirectional, two dimensional or three dimensional arrangements of fibers. The properties in any direction will be proportional to amount of fibers in that direction. [2]

2.3.3. Applications of FRP'S

Development of FRPs can be considered as one of the biggest advances in material technology in the 20th century. It has found its applications in many fields for instance medicine, communication engineering and other industries. FRPs are also being introduced in the construction industry. Significant research is being conducted in exploring the various uses of FRP in the field of construction. [5] Considerable progress in application of FRPs in bridge engineering has been achieved. One of the most promising applications of FRP in structural engineering appears to be repair and rehabilitation of different members such as beams and columns. The success of structural rehabilitation measures have led to development of new lightweight structural concepts utilizing all FRP systems or new FRP/concrete composite system

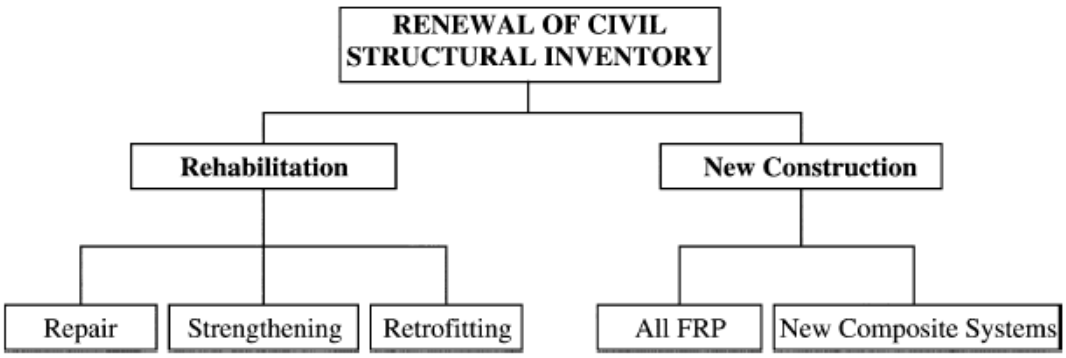

Figure 2.2: Use of FRP Composite in Civil Engineering [4]

(a)

(b)

(c)

Figure 2.3: Application of FRP to a bridge [5]

2.4 Fiber Types

The most common fiber types used in composite industry are glass, carbon and organic (Kevlar). Boron, silicon carbide (SiC), alumina and other fibers are used in specialized applications.

2.4.1 Glass Fibers

Glass fibers exhibit the typical glass properties of hardness, corrosion resistance, and inertness. They are flexible, lightweight, and inexpensive. These properties make glass fibers the most common type of fiber used in low cost industry applications. Because glass has an amorphous structure, its properties are the same along the fiber and across the fiber. Glass fibers are useful because of their high ratio of surface area to weight. The high strength of glass fibers is attributed to the low number and size of defects on the surface of the fiber. Tensile strength of glass fibers reduces at elevated temperature but can be considered constant for the range of temperature at which polymer matrices can be exposed (upto 275ºC depending on the matrix type). Glass fiber are shown in figure 2.4

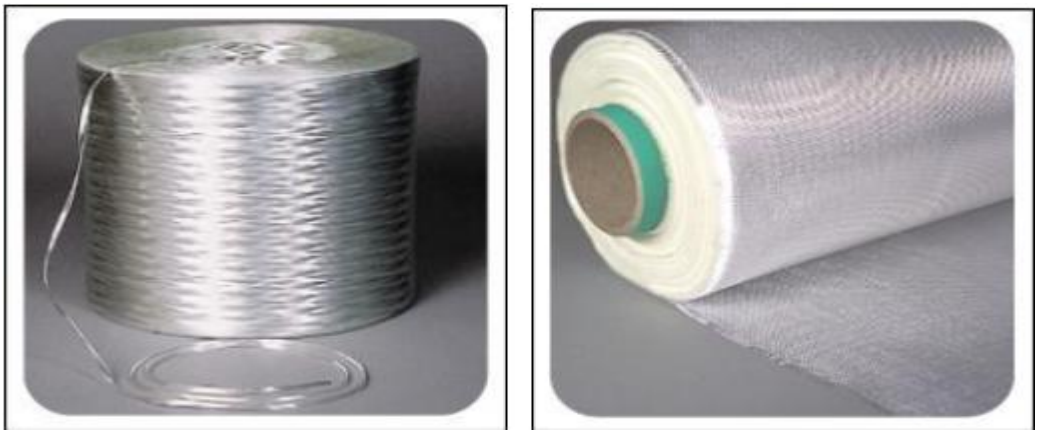

(a) (b)

Figure 2.4: (a) Roll of Glass fiber (b) Woven Fabric of Glass fiber [6]

2.4.2 Carbon Fibers

A carbon fiber composite refers to a composite in which at least one of the fillers is carbon fibers, short or continuous, unidirectional or multidirectional, woven or nonwoven. The matrix is usually a polymer, a metal, a carbon, a ceramic, or a combination of different materials. Except for sandwich composites, the matrix is three-dimensionally continuous, whereas the filler can be three-dimensionally discontinuous or continuous. The properties of carbon fibers depend on the raw material and manufacturing process. The fibers begin as an organic fiber, rayon, polyacrylonitrile or pitch which is called the precursor. The precursor is then

stretched, oxidized, carbonized and graphitized. There are many ways to produce these fibers, but the relative amount of exposure at temperatures from 2500-3000°C results in greater or less graphitization of the fiber. Higher degrees of graphitization usually result in a stiffer fiber (higher modulus) with greater electrical and thermal conductivity values.

Figure 2.5: Roll of Carbon fiber [6]

2.4.3 Aramid Fibers

The best known organic fibers are aramid fibers. Aramid fibers have high energy absorption during failure, which makes them ideal for impact and ballistic protection. Because of their low density, they offer high tensile strength-to-weight ratio, and high modulus-to-weight ratio, which makes them attractive for aircraft and body armour. Aramid composites have relatively poor shear and compression properties. Careful design is required for their use in structural applications that involve bending or compression.

Figure 2.6: Roll of Aramid fiber [6]

2.5 Glass Fiber Reinforced Polymer

In the present work GFRP are used and therefore, further GFRP is describes in following section.

Glass fiber reinforced polymers sheets are being increasingly used in rehabilitation and retrofitting of concrete structures as an alternative to steel in concrete due to their high strength to weight ratio and corrosion and fatigue resistance. Ease of handling and application at site are its added advantage.

Of the different type of glass fibers, E-glass is mostly used for reinforcement due to its high strength and electrical resistivity. Glass fibers have high strength and temperature resistance, but it is low cost that makes the GFRP the most popular FRP reinforcement in civil engineering applications. GFRP's have been found attractive in Asian region due to their cost competitiveness over carbon fiber composites.

The FRP sheets are being used for repair, strengthening and retrofitting of structural components. Degradation of steel reinforcements due to corrosion, cracking of concrete due to weathering, rapidly changing traffic needs (both in terms of intensity and load levels) and recent earthquake damages have necessitated the use of strengthening of basic structural components such as slabs, panels, walls, beams and columns. Tests carried on concrete beams reinforced externally with FRP plates indicate substantial increase in the strength of the beams and decks. Wrapping of columns with FRP have been studied for enhanced performance and are found suitable for seismic column retrofitting. Wide spread utilization of FRP's in construction is hampered by lack of long-term durability and performance data in tropical environment.

The main environmental factors for the deterioration of GFRP are temperature, sunshine, water/moisture, alkalinity resulting from hydration of cement in concrete and stress due to service loads. Most of the early durability tests carried out on GFRP was for applications in auto and aerospace industries. The durability data with reference to one or combinations of some of these parameters is presently available. Beams bonded externally with GFRP sheet and subjected to wet and dry exposure under sea water resulted in 33% reduction in strength.

Hence in this chapter we have studied the basics of FRP composites, various adverse effects of moisture over GFRP which can further propagate the damage over whole FRP structure and water which can delaminate the Glass fiber and matrix.

In the next chapter we are going to discuss some of theoretical and experimental work done by various researchers to study the effect of moisture absorbed over resonant frequency, effect of defects at concrete-fiber interface and effect of delamination at fiber-epoxy-fiber interface.

Chapter 3

Literature Review

The present chapter represents the review of some of experimental and theoretical work done by various researchers in the field of GFRP composites for measuring the moisture absorption, defect detection, delamination by using coplanar strip lines capacitance calculation.

3.1 Effect of Water Absorption on Dielectric Constant

P. Thomas et al. [7] studied the water absorption characteristics of three glass-epoxy polymer composite systems. Composites having three different volume fractions of fibers were fabricated using the hand layup technique by stacking two different fabrics, chiefly, woven roving (WR) and chopped stand mat (CSM). While for one set, the top layer was made of CSM and the bottom WR (Composite l), that for the next two, CSM layers were both at the top and bottom while the number of WR that followed these cover layers was either two in one case (Composite 2) or three in other (Composite 3). The dielectric dissipation factor, dielectric constant and insulation resistance measurements were carried out on these composites at room temperature as well as after subjecting to water absorption up to 96 h.

The weight gain for all three types of composites show a linear increasing trend up to 72 h and after that a trend for saturation sets in. Further, it is seen that the dielectric dissipation factor and dielectric constant of the composites increase with increase in the water absorption duration and correspondingly the insulation resistance shows a deteriorating trend. Among the three composites studied, Composite 2 having highest fiber content and hence the least matrix content shows better performance compared to composites 1 and 3.Very small amount of moisture ingress in the composite materials has significant effect on the electrical properties. The moisture absorption acts as carriers of electrical charges and hence increases the leakage current, increases the dielectric dissipation.

Dakhakhni et al. [8] introduced a new concept for detecting air voids, water intrusion, and glue infiltration damages in fiber reinforced polymers (FRPs)-

strengthened concrete structures. The concept, based on detecting the local dielectric permittivity variations, was employed to design coplanar capacitance sensors (CCSs) to detect such defects. An analytical model was used to introduce the sensor operation theory and analyze the influence of different sensor parameters on the output signals and to optimize sensor design. Two dimensional finite element (FE) simulations were performed to assess the validity of the analytical results and to evaluate other sensor design-related parameters. To experimentally verify the FE model, dielectric properties of various materials involved in FRP-strengthened concrete systems were measured. In addition, two concrete specimens strengthened with FRP laminates and containing pre-induced defects were constructed and inspected in a laboratory setting. Good agreement was found between experimental capacitance measurements and those predicated by the FE simulations. The proposed CCS design, coupled with commercially available portable capacitance meters, would facilitate field implementation of the proposed technique for rapid inspection of FRP-strengthened concrete structures without the need for sophisticated data analyses usually required by other more expensive and time consuming methods.

Yin et al. [9] describes the application of capacitive imaging to the inspection of concrete. A two-dimensional finite-element method was employed to model the electric field distribution from capacitive imaging probe, and how it interacts with concrete samples. Physical experiments with prototype capacitive imaging probes were also carried out. The proof of concept results indicated that the capacitive imaging technique could be used to detect cracks on the surface of concrete samples, as well as sub-surface air voids and steel reinforcement bars.

3.2 Correlation of Moisture and Capacitance

G. D. Davis et al. [10] used electrochemical impedance spectroscopy (EIS) sensors to inspect carbon fiber reinforced polymer (CFRP) -reinforced concrete structures exposed to a variety of test conditions. Similar specimens were also used to investigate the detection of delamination between the CFRP and the concrete using a modified wedge test configuration. The use of external electrodes attached to the CFRP surface, coupled with the embedded rebar, provided the best results. Equivalent circuit modelling was used to analyze the impedance spectra. Several circuit parameters, especially the capacitance and constant phase element (CPE) magnitude,

correlated very well with both bonded area/delamination and moisture. Both parameters exhibit a linear relationship with delamination area. The capacitance also showed a linear relationship with moisture content while the CPE was more strongly dependent on moisture. Differences in the response of the specimens subjected to the different exposure conditions were seen and explained based on the moisture uptake of the various specimens.

Y. Shimamura et al. [11] proposed a new method to measure the moisture absorption ratio of FRP by the change of the dielectric constant, which corresponds to the capacitance, of a micro polyimide sensor embedded in FRP is proposed. At first, the relationship between the moisture absorption ratio and the dielectric constant change of the sensor itself is investigated. Then, GFRP specimens in which the sensor is embedded in the mid plane are immersed in water, and the moisture absorption ratio of the specimen and the dielectric constant change of the sensor are monitored.

3.3 Correlation of Moisture and Return loss

Mirjana Bogosonavich et al. [12] proposed a technique for the measurement of the permittivity of homogeneous dielectric materials using micro strip patch antenna sensor. In this method we put the antenna in different mediums and observed the reflection coefficient from the medium and see the change in the resonant frequency of the antenna.

A. Cataldo et al. [13] proposed the different approaches and techniques that are commonly available for the continuous monitoring of moisture levels and dielectric properties of materials. He studied the feasibility of the adoption of the time-domain reflectometry analysis for such purposes, using a patch antenna as sensing element. This way, the extrapolation of the scattering parameters is suitably correlated to the water content levels of the materials under test.

R. Wakodkar et al. [14] proposed a method in which the effect on the resonant frequency of a rectangular microstrip patch antenna due to the accumulation of water over its microstrip patch surface. With the increase in the moisture ingress, resonant frequency decreases.

3.4 Defect detection in Concrete Structures

Shams et al. [15] proposed that infrastructure health monitoring using embeddable wireless sensors has drawn considerable attention lately. Such sensors will need antennas to support data communication as well as wireless power reception functions. In this paper the gain and return loss properties of an embedded microstrip patch antenna within concrete are studied as function of the air-gap and concrete cover thickness. The transmission between one antenna in free-space and another embedded within concrete are measured to demonstrate the feasibility of wireless power transmission to the embedded sensor.

Maria Q. Feng et al. [16] the authors develop an electromagnetic (EM) imaging technology for detecting voids and debonding between the jacket and the column, which may significantly weaken the structural performance of the column otherwise attainable by jacketing. This technology is based on the reflection analysis of a continuous EM wave sent toward and reflected from layered FRP-adhesive-concrete medium: Poor bonding conditions including voids and debonding will generate air gaps which produce additional reflections of the EM wave. In this study, dielectric properties of various materials involved in the FRP-jacketed RC column were first measured. Second, the measured properties were used for a computer simulation of the proposed EM imaging technology. The simulation demonstrated the difficulty in detecting imperfect bonding conditions by using plane waves, as the scattering contribution from the voids and debonding is very small compared to that from the jacketed column. Third, in order to alleviate this difficulty, a special dielectric lens was designed and fabricated to focus the EM wave on the bonding interface. Furthermore, the time gating technique is used in order to reduce the noise resulting from various uncertainties associated with the jacketed columns. Finally, three concrete columns were constructed and wrapped with glass-FRP jackets with various voids and debonding condition artificially introduced in the bonding interface. Using the proposed EM imaging technology with the lens especially designed and installed, these voids and debonding condition were successfully detected.

Afzal, Shahid Kabir [17] proposed that fiber optic sensors are being extensively developed and utilized in various fields, compared to conventional sensing technologies, due to their exclusive properties, such as complete immunity to

electromagnetic interference, capability of functioning in hostile surroundings, elevated sensitivity and user friendliness. The unique characteristics of fiber optic sensors can provide more accurate and precise detection of crack damage in concrete structures, the deterioration of which is one of the major growing problems worldwide.

3.5 Coplanar Strip line parameters calculation

Chen Erli et al. [18] derived wave parameters of coplanar transmission lines expressed in analytical formulas using conformal mapping. The accuracy of these formulas was verified experimentally on variety of coplanar transmission lines using differential electro-optic (DEOS) sampling.

S Gevorgian et al. [19] derived improved closed form formulas for the basic parameters of one and two layer substrate CPS. The dielectric constant of the layer between the strips and substrate should not be smaller than the dielectric constant of the substrate, e2 > e1. For e2 < e1 the magnetic wall approximation at the dielectric/dielectric interfaces is violated , and the accuracy of above approximation is very poor.

S. Gevorgian et al. [20] proposed a simple method and closed-form analytic formulas for symmetric CPS based on single layer substrate (infinite and finite thickness) and multilayer lossy dielectric (semiconductor) substrate, where the permittivity of the superstrate layers decrease away from the strips, are proposed. Since the line models are given analytically, the dependencies of the line parameters may be analyzed and optimized in wide ranges of sizes, permittivities, and losses (substrate resistivity). In general, the formulas are reversible. The measured line parameters (Z; ε_{eff}; α) may be used to calculate the permittivity and loss tangent (resistivity) of one of the substrate layers if the parameters of the other layers and strips are known. The method may be easily extended to include larger number of substrate layers.

Chapter 4

Defect detection in Concrete and Study of Delamination using CPS

This chapter presents the theoretical, simulated results and an experimental program undertaken to investigate the presence of defects between the concrete and GFRP using CPS. The entire experimental program consisted of tests on three delamination sheets and three GFRP wrapped concrete specimens. The simulated and experimental results are presented here for discussion. The specimens were tested using the LCR meter to find the capacitance of CPS. The presence of defects was measured by finding the change in the capacitance of Coplanar Strip at low frequency. The following sections discuss the problem formulation, fabrication of FRP and Concrete samples and results obtained from the simulations and experimentation using CPS.

4.1 Problem formulation

Fiber Reinforced Polymer (FRP) is a relatively new class of composite material manufactured from fibers and resins, and has proven efficient and economical for the development and repair of new and deteriorating structures in civil engineering. The mechanical properties of FRPs make them ideal for widespread applications in construction worldwide. FRPs have been used widely by civil engineers in the design of new construction. Structures such as bridges and columns built completely out of FRP composites have demonstrated exceptional durability, and effective resistance to effects of environmental exposure. Prestressing tendons, reinforcing bars, grid reinforcement, and dowels are all examples of the many diverse applications of FRP in new structures. One of the most common uses for FRP involves the repair and rehabilitation of damaged or deteriorating structures. Several companies across the world are beginning to wrap damaged bridge piers to prevent collapse and steel-reinforced columns to improve the structural integrity and to prevent buckling of the reinforcement.

In the all above uses FRP is exposed to all harsh conditions, and various environmental conditions in the presence of moisture. The deterioration that occurs in FRP during the service life in general, is linked to the poor workmanship and the presence of defects that is occurred, which can initiate undesirable structural changes

within the fiber reinforcement and the matrix or the interface between the two. It can further lead to moisture ingress into concrete cover and hence lead to corrosion steel reinforcement. Hence it is necessary to detect moisture ingress as soon as possible.

In the present work water and air void are found in Glass Fiber Reinforced Polymer (GFRP) Woven Fabric (E Glass) wrapped concrete structure in terms of capacitance of CPS and electric field of the specimen. The changes in the value of capacitance of the specimen and electric field distribution of that specimen under natural conditions have also been studied.

4.2 Flow chart for work done

The moisture absorption and defect detection in GFRP is found in 3 ways as shown in the flow chart given in Figure 4.1

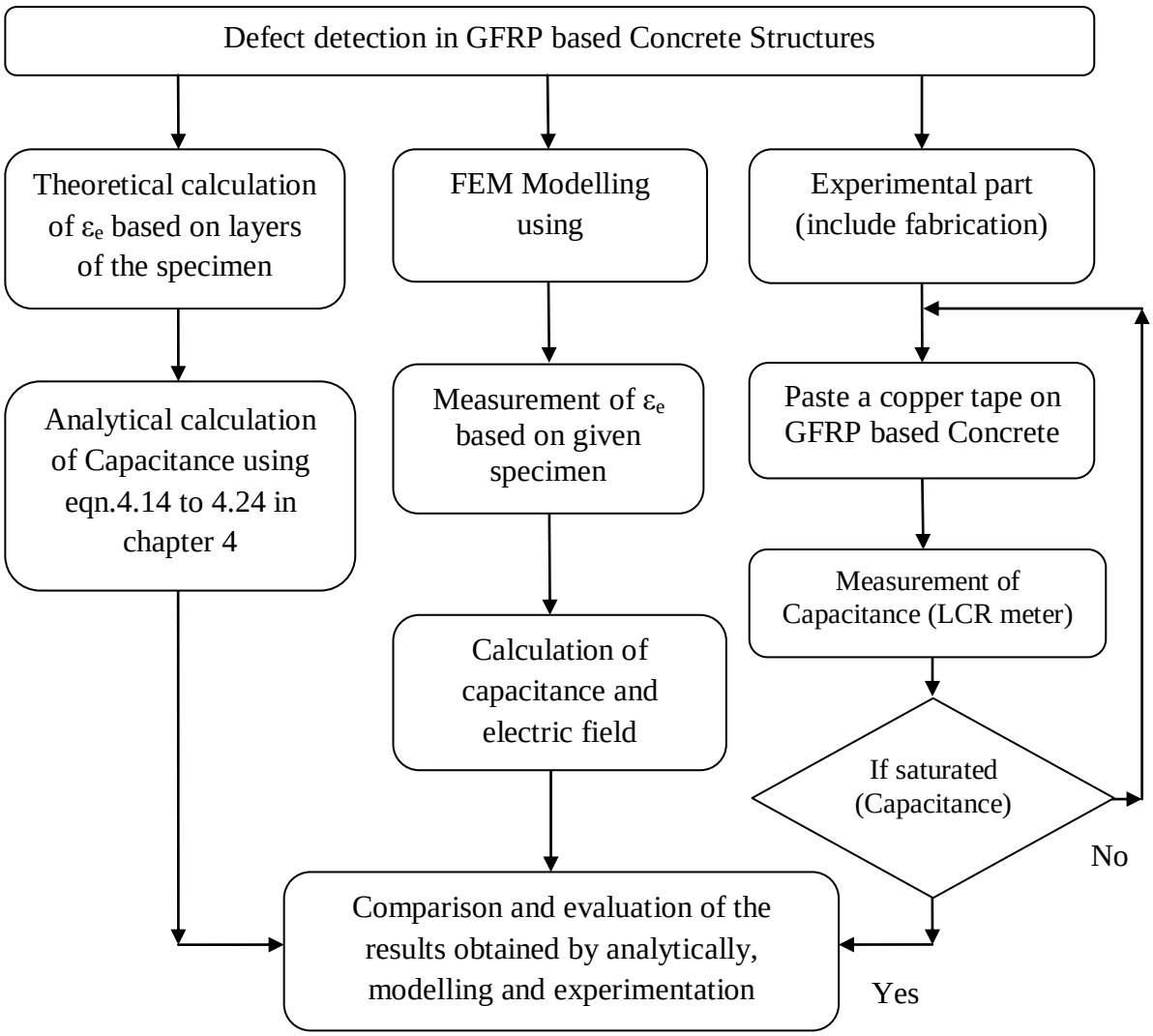

Figure 4.1Flow chart for the work done

4.3 Mathematical analysis

The proposed analysis relies on detecting the variation of dielectric signatures in material compositions of the composite parts. The change in dielectric permittivities as a result of damage, inside the composite material would produce a change in the measured capacitance and electric field at low frequency. That's why CPS method is used here for analysis of capacitance.

4.3.1 Coplanar Strip lines

The coplanar stripline (CPS) consists of a dielectric substrate with two parallel strip conductors separated by a narrow gap as shown in Figure 4.2. This basic structure is referred to as the conventional CPS.

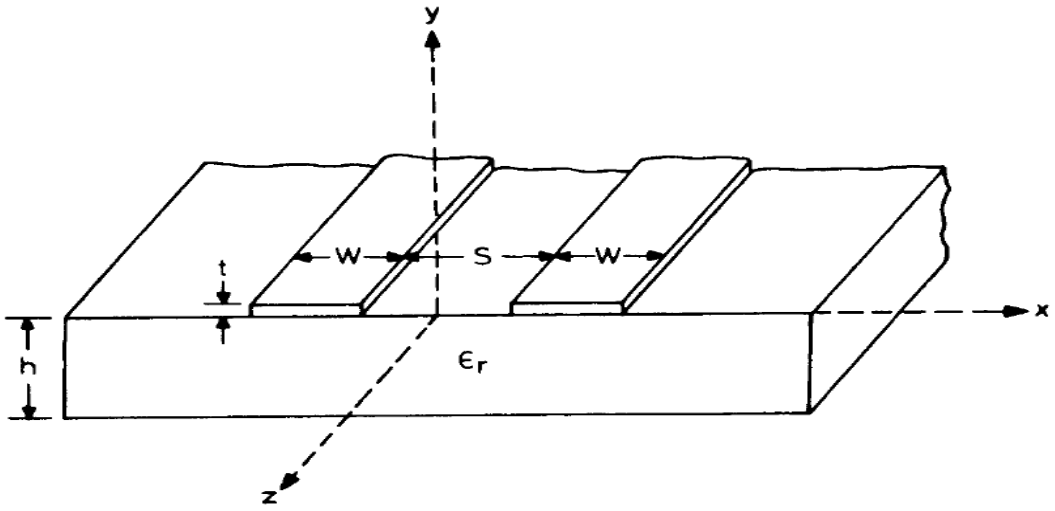

Figure 4.2: Coplanar Strip Geometry [21]

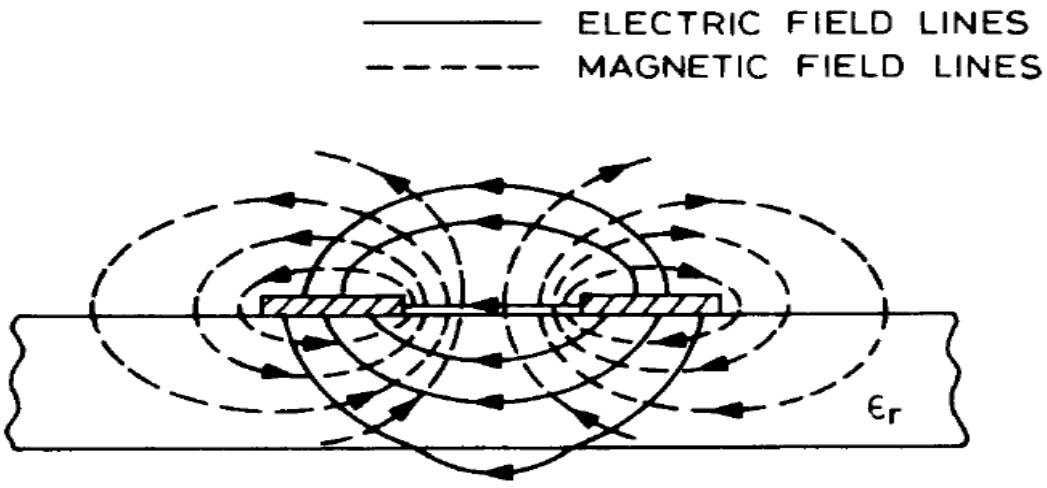

Figure 4.3: Electric and Magnetic field distributions in CPS [21]

Symmetric (two strips are identical) CPS is inherently balanced, i.e., the currents in the strips are opposite but equal and have similar distributions across the strips. Due to the balanced nature, the lines are less sensitive to induced noises and are widely used in low-noise amplifiers, oscillators, etc. They are especially useful as transmission lines/interconnects for high-loss substrates, e.g., silicon. If the cross-sectional dimensions are chosen properly, these lines provide lower substrate losses since the currents induced in the substrate may be partially cancelled, thus reducing the losses in the substrate.

The advantages of CPS are as follows: (1) Series as well as shunt mounting of devices is possible. (2) The CPS is a balanced transmission line. Hence its applications include balanced mixers and feed network work for printed dipole antennas. The main disadvantage of the CPS is that because it lacks a ground plane. The line can support besides the fundamental CPS mode two other parasitic modes, namely the TE0 and TM0 dielectric slab waveguide modes. These parasitic modes do not have a cut off frequency. The TE0 and TM0 modes have their electric fields predominantly parallel and perpendicular to the dielectric ε_r air interface, respectively. The electric field of the fundamental CPS mode is predominantly parallel to the dielectric ε_r air interface and hence strongly couples to the TE0 parasitic mode at discontinuities [20].

4.3.2 Equivalent circuit of CPS

The equivalent circuit of a CPS is given in Figure 4.4. For the per unit length line parameters shown in Figure 4.4, the line impedance and propagation constant are given by:

$$Z = \sqrt{\frac{r + j\omega L}{G + j\omega C}} \tag{4.1}$$

$$\gamma = \sqrt{(r + j\omega L)(G + j\omega C)} \tag{4.2}$$

Conformal mapping and partial capacitance techniques are extensively used to derive closed form analytical expressions for C, L, and G parameters. A simple

approximation can be used for R. In Figure 4.4, R is the resistance of CPS, G is the conductance, L is inductance and C is capacitance of a CPS per unit length.

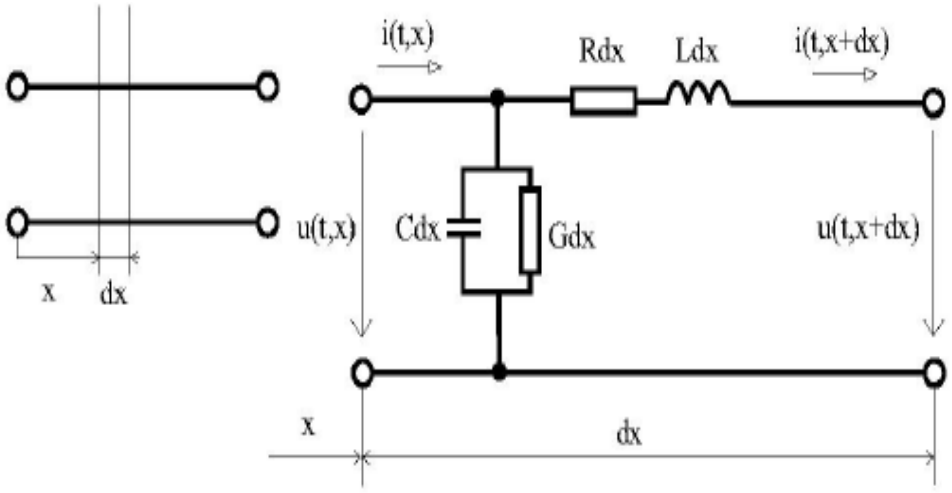

Figure 4.4 Equivalent Circuit of CPS [22]

4.4 Analysis of CPS

4.4.1 Single layer Substrate CPS

The sequence of conformal transformations for a finite thickness substrate CPS is shown in Figure 4.5. The substrate is assumed to have dielectric constant ε and thickness h. The width of the strips is s, and the spacing between them is 2g, Figure 4.5. First, we evaluate the partial capacitance due to dielectric slab with an equivalent dielectric constant (ε-1) [23], [24], [25]. The symmetry plane at x=0 is regarded as an electric wall, while the dielectric/air interfaces are approximated by magnetic walls. Then the capacitance between the strips is the capacitance of series connected between the strips and the electric wall capacitors, Figure 4.5 a). In the first step the semi-infinite right hand side of the dielectric strip with a thickness h and equivalent dielectric permittivity (ε-1) in the Z-plane Figure 4.5 a), is mapped on a lower part of T-plane, Figure 4.6 a) using transformation $t = \cos h^2\left(\frac{\pi z}{2h}\right)$. This mapping results in the following vortex coordinates in T plane:

$$t_1 = 1;\ t_2 = \cos h^2\left(\frac{\pi g}{2h}\right);\ t_3 = \cos h^2\left(\frac{\pi(s+g)}{2h}\right);\ t_4 = t_5 = \infty;\ t_6 = 0$$

a) b)

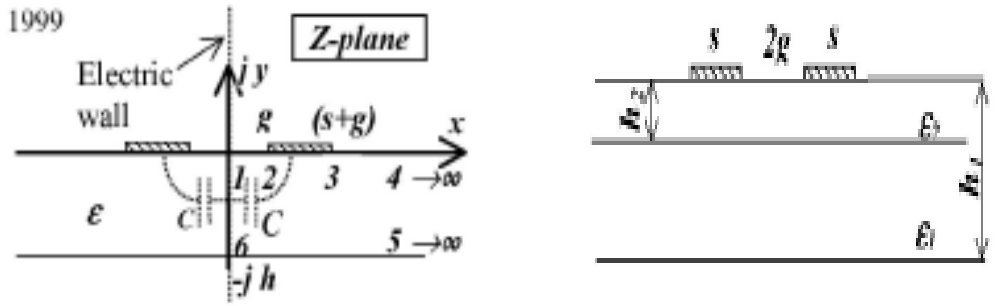

Figure 4.5 (a) Single layer substrate (b) Double layer substrate CPS

The lower part of the T-plane is mapped on a rectangle in W-plane, shown in Figure 4.6.b), using Schwartz-Christoffel transformation. For coordinates given above ($t>t_3>t_2>t_1->t_6$) the modulus of the complete elliptic integral [26] (p.72, 1.2.23) may be transformed to

a) b)

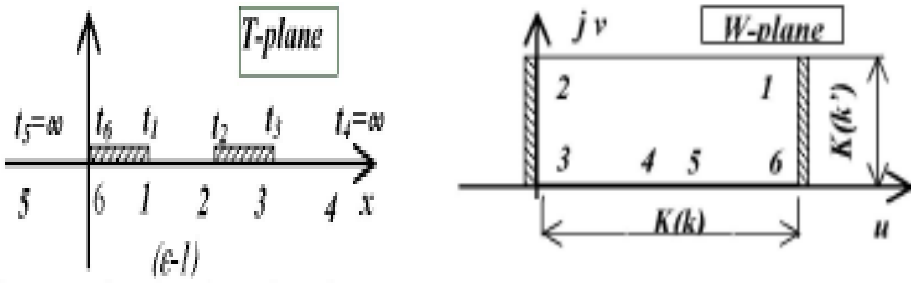

Figure 4.6 Sequence of conformal transformations

$$k = \frac{\tanh(\frac{\pi g}{2h})}{\tanh(\frac{\pi(s+g)}{2h})} \qquad (4.3)$$

From the last transformation $w_1=K(k)+jK(k)$, Figure 4.6 b). Then the capacitance of the parallel-plate capacitor, Figure 4.6 b), is:

$$C = \in_0 (\in -1)\frac{K(k')}{K(k)} \qquad (4.4)$$

K(k) and jK(k') complete elliptic integrals of the first kind with $k' = \sqrt{1-k^2}$. A similar capacitance is due to the left-hand side of Figure 4.5 a), hence the total partial capacitance due the substrate is:

$$C_s = \in_0 (\in -1)\frac{K(k')}{2K(k)} \qquad (4.5)$$

The partial capacitance between the two strips (air above and below), Figure 4.5 a), in the absence of the substrate is derived from (3) at h=∞ limit, assuming (ε-1) =1:

$$C_a = \in_0 \frac{K(k_o')}{K(k_o)} \tag{4.6}$$

Where

$$k_o = \frac{g}{s+g}, \qquad k_o' = \sqrt{1 - k_o^2}$$

Finally, the total line capacitance, Figure 3.4 a), is $C=C_s+C_a$

$$C = \in_0 \in_{eff1} \frac{K(k_o')}{K(k_o)} \tag{4.7}$$

with an effective dielectric constant and filling factor defined as: $\in_{eff1} = 1 + (\in -1)q$

$$q = \frac{1}{2}\frac{K(k')}{K(k)}\frac{K(k_o')}{K(k_o)} \tag{4.8}$$

The impedance of a finite thick substrate CPS is

$$Z = \frac{120\pi}{\sqrt{\in_{eff1}}}\frac{K(k_o')}{K(k_o)} \tag{4.9}$$

4.4.2 Two Layer Substrate CPS

In this case, we assume air above the strips and below the substrate, Figure 4.6 b). It is assumed that the dielectric permittivity of the additional layer is larger than the dielectric permittivity of the substrate. The total line capacitance of this CPS may be written as a sum of partial capacitances, $C = C_a + C_1 + C_2$ where Ca is the capacitance between the strips in the absence of dielectric layers (4). C1 and C2 are the partial capacitances of the dielectric layers with equivalent dielectric constants (ε_r-1) and (ε_2-ε_1), and thickness h_1 and h_2 respectively [27]. The resulting capacitance of a two layer substrate CPS is

$$C = \in_0 \in_{eff2} \frac{K(k_o')}{K(k_o)} \tag{4.10}$$

with an effective dielectric constant, $\in_{eff2} = 1 + (\in_1 - 1)q_1 + (\in_2 - \in_1)q_2$. The filling factors, associated modulus of the elliptic integrals and the impedance of this CPS are given as:

$$q_i = \frac{1}{2}\frac{K(k_i')}{K(k_i)}\frac{K(k_o')}{K(k_o)}; \qquad i = 1,2 \tag{4.11}$$

$$k_i = \frac{\tanh\left(\frac{\pi g}{2h_i}\right)}{\tanh\left(\frac{\pi(s+g)}{2h_i}\right)} \qquad i = 1,2 \tag{4.12}$$

$$Z = \frac{120\pi}{\sqrt{\in_{eff2}}}\frac{K(k_o)}{K(k'_o)} \tag{4.13}$$

4.4.3 Multilayered Layered Substrate CPS

For a multilayered structure given in figure 3.6, the effective dielectric constant can be expressed as

$$\in_{re} = q_1 \in_{r1} + q_2 \in_{r2} + q_3 \in_{r3} + \ldots\ldots\ldots\ldots + q_n \in_{rn} \tag{4.14}$$

where $q_1, q_2 \ldots\ldots, q_n$ describe the filling factors for the various dielectric regions. To illustrate how to obtain the filling factors for a multilayered CPS we should know about the double layered CPS configuration which is given in section 4.4.2.

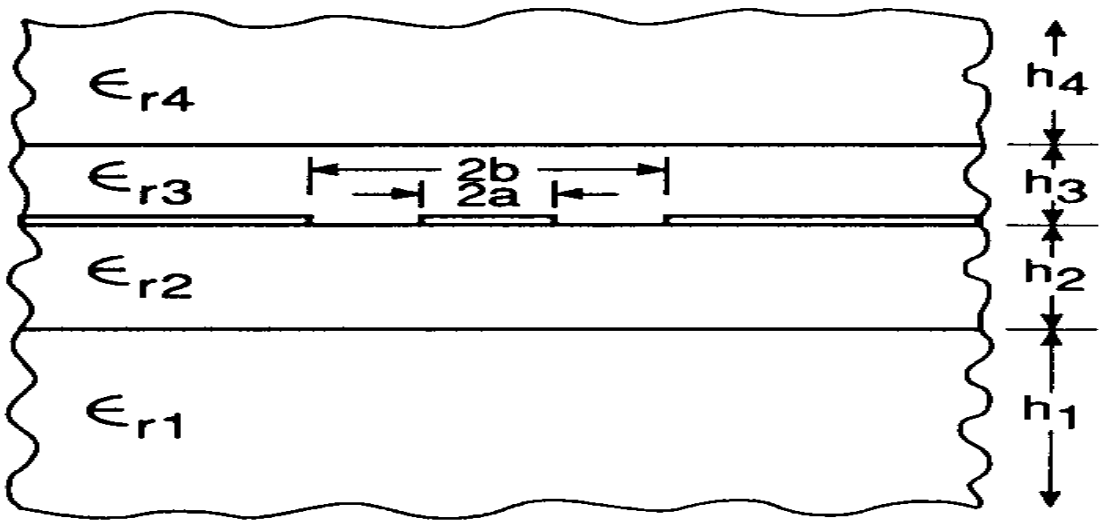

Figure 4.7 Multilayered CPS [21]

The general expression for the capacitance of the *i*th layer with dielectric replaced by air is

$$C_{si}^{a} = 2 \in_0 \frac{K(k_i)}{K'(k_i)} \tag{4.15}$$

where

$$k_i = \begin{cases} \dfrac{a}{b} & \text{for the half plane} \quad (4.16a) \\ \dfrac{\sinh\left(\frac{\pi a}{2h}\right)}{\sinh\left(\frac{\pi b}{2h}\right)} & \text{for a dielectric layer of thickness h} \quad (4.16b) \\ \dfrac{\tanh\left(\frac{\pi a}{2h}\right)}{\tanh\left(\frac{\pi b}{2h}\right)} & \text{for a dielectric layer backed by a conductor} \quad (4.16c) \end{cases}$$

Let us now determine the filling factors for the four layered configuration in figure 4.7 In this case,

$$C^{a} = 4 \in_0 \frac{K(k)}{K'(k)}, \quad k = \frac{a}{b} \tag{4.17}$$

The filling factor for the second layer, is

$$q_2 = \frac{C_{s2}^{a}}{C^{a}} \tag{4.18}$$

with

$$C_{s2}^{a} = 2 \in_0 \frac{K(k_2)}{K'(k_2)}, \qquad k_2 = \frac{\sinh\left(\frac{\pi a}{2h_2}\right)}{\sinh\left(\frac{\pi b}{2h_2}\right)} \tag{4.19}$$

Similarly,

$$q_3 = \frac{C_{s3}^{a}}{C^{a}} \tag{4.20}$$

with

$$C_{s3}^{a} = 2 \in_0 \frac{K(k_3)}{K'(k_3)}, \qquad k_3 = \frac{\sinh\left(\frac{\pi a}{2h_3}\right)}{\sinh\left(\frac{\pi b}{2h_3}\right)} \tag{4.21}$$

For the top most layer, the filling factor is defined as

$$q_4 = \frac{\frac{C^a}{2} - C_{s3}^a}{C^a} = \frac{1}{2} - \frac{C_{s3}^a}{C^a} \qquad (4.22)$$

Similarly, for the lowest layer

$$q_1 = \frac{\frac{C^a}{2} - C_{s2}^a}{C^a} = \frac{1}{2} - \frac{C_{s2}^a}{C^a} \qquad (4.23)$$

It can be verified that

$$q_1 + q_2 + q_3 + q_4 = 1 \qquad (4.24)$$

The above analysis can be extended to any number of dielectric layers in CPS.

In our work, capacitance is calculated using CPS method for three layer of GFRP wrapped concrete specimen and five layers of delamination sheet but this approach is applicable to only without void detection and lack in to find the capacitance of defected zone in samples.

4.5 FEM Modelling

In this modelling, artificially model of the specimen is created and run the model in the Maxwell 2d software which gives the value of the capacitance and electric field distribution of the model.

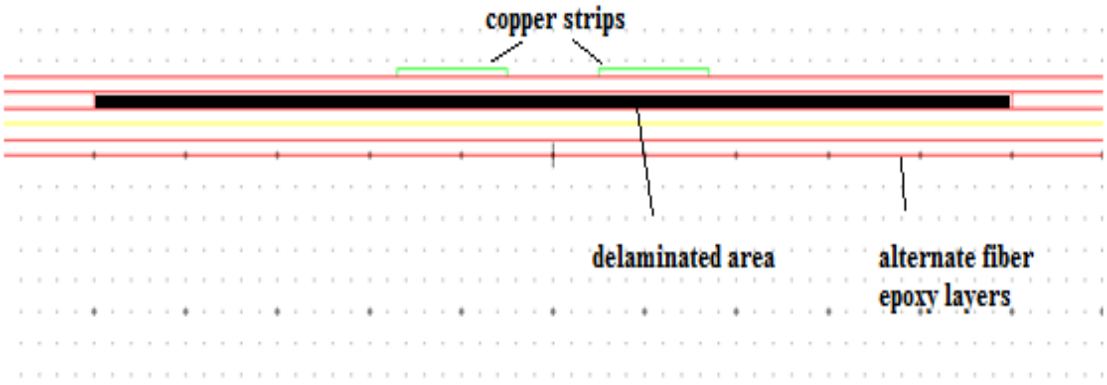

Figure 4.8 Model of delamination in fiber-epoxy-fiber layers

In section 4.9, simulated results of delamination are given in detail.

4.6 Experimental set up

The set up basically consist of following main items:-

Table 4.1 List of items used in experimental set up

ITEM NAME	QUANTITY
LCR Meter	1
Copper tape roll	1
Concrete slabs	3
Delamination samples	3

4.7 Fabrication of FRP and Concrete Samples

GFRP samples were made using woven glass fabric of 50 cm width having 0º fiber orientation woven with polymer fibers (Figure 5.2). Then in order to make glass fabric a composite material epoxy resin (by M Brace) was used. Epoxy consists of (i) Base and (ii) Hardener. Base is the main ingredient and hardener is mixed in ratio of 100: 40 respectively.

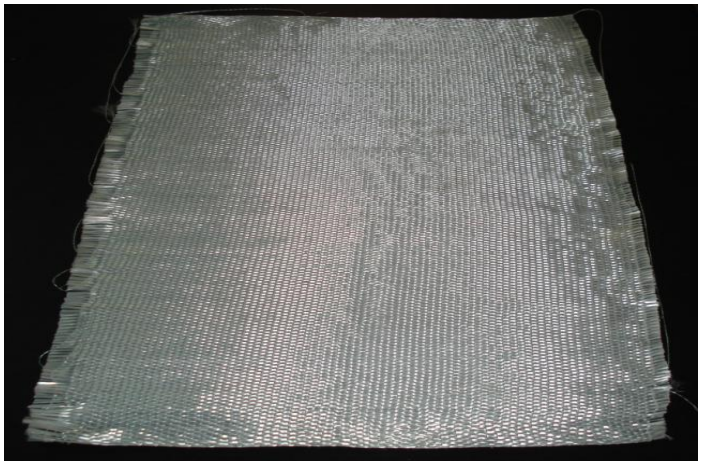

Figure 4.9 Uncoated GFRP sheet used

Then in order to make glass fabric a composite material epoxy resin (by M Brace) was used. Epoxy consists of (i) Base and (ii) Hardener. Base is the main ingredient and mixed in ratio of 100: 40 respectively. The FRP sheet was taken and the epoxy resin is uniformly applied on one side of glass fiber and took overnight to dry and now coat was applied to another side of sheet which makes single layer GFRP. For Three layer GFRP same layer (epoxy:glass:epoxy) is sand-witched three times.

(a)

(b)

Figure 4.10 (a) GFRP sheet being resin coated (b) fully cured sheet with epoxy coating

The fully cured concrete slab was prepared with size of 300x300x65mm^3 using wooden moulds as shown in Figure 4.10. Now symmetric copper strips of 12x300mm^2 are pasted on samples with a gap of 10mm as shown in Figure 4.11.

(a)

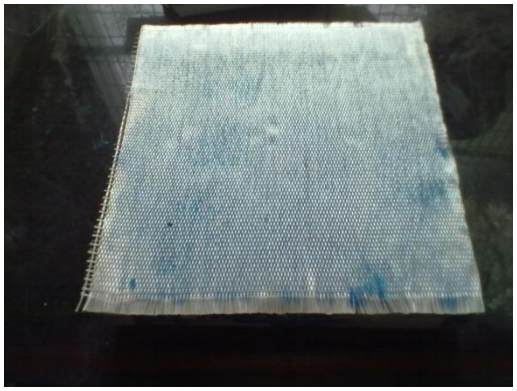

(b)

Figure 4.11(a) wooden mould to make concrete slab (b) Concrete wrapped with GFRP

Figure 4.12 GFRP wrapped concrete with copper strips

(a)

(b)

(c)

Figure 4.13 Samples of Delamination of Size: (a) 50x55mm^2 with CPS (b) 50x105mm^2 with CPS (c) 50x155mm^2 with CPS

4.8 Testing of samples

4.8.1 Testing of delaminated samples

Firstly to find the delamination at glass epoxy interface, created the delamination at that surface and measured it with the help of LCR meter and then compared with the capacitance value calculated from the modelling. As the length of the delamination sheet increases the value of capacitance is increases experimentally as well as in modelling using Maxwell 2D.

(a)

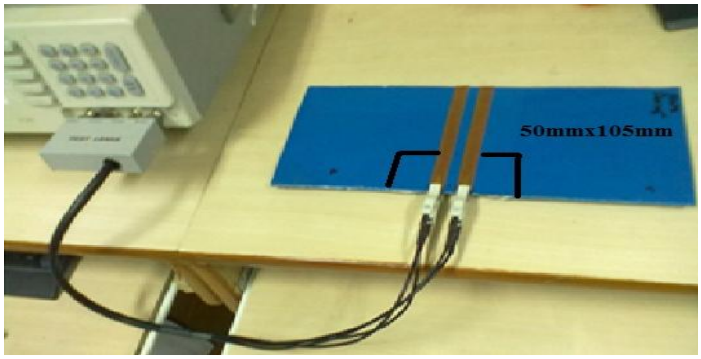

(b)

(c)

Figure 4.14 Testing of delaminated samples: (a) Sample 1 (b) Sample 2 (c) Sample3

4.8.2 Testing of GFRP wrapped concrete samples

To find out the presence of defect in GFRP wrapped concrete structures, created the defect artificially on the concrete epoxy interface and measured the capacitance using LCR meter and compared it with the simulated value of capacitance from the modelling on Maxwell 2D.

(a)

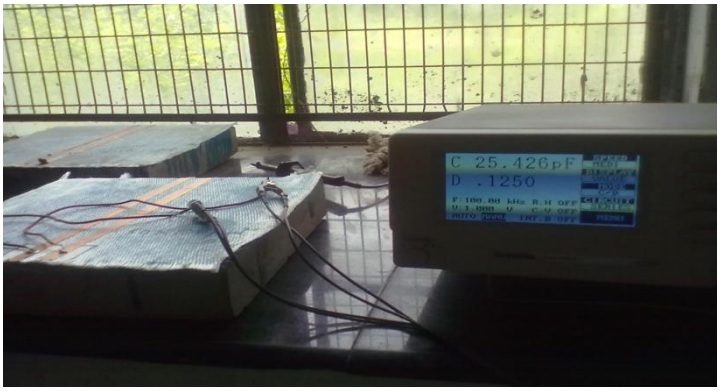

(b)

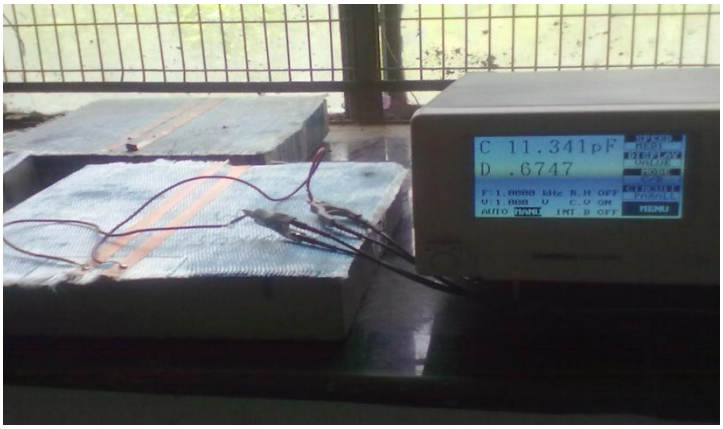

(c)

Figure 4.15 Testing of GFRP wrapped concrete structures (a) without any void (b) with void of size 50x60mm^2 (c) with void of size 50x100mm^2

4.9 Effect of Delamination in fiber-epoxy-fiber sheet over Capacitance

Layered fiber reinforced composite materials are susceptible to crack initiation and growth in the resin rich layer between plies. These cracks, more commonly referred to as delaminations, represent one of the most prevalent life-limiting failure modes in laminated composite structures. Delamination may arise from extremities of reinforcement (end debonding) or from intermediate cracks in the concrete. [28],[29]

We observed that as the length of the delamination in sheet increases, the value of capacitance is increases experimentally as well as in modelling using Maxwell 2D.

Table 4.2 show the variation in capacitance with the increase in the length of the de-lamination in the sheets.

Delaminated Samples	Simulated results using Maxwell 2D	Theoretical Value Without void
Change in area (mm^2)	Change in Capacitance (pf)	Capacitance (pf)
1. No Void	4.9882	6.077
2. 50x55	6.9983	-
3. 50x105	7.6938	-
4. 50x155	9.6606	-

Table 4.3 show the variation in capacitance with the increase in the length of the de-lamination in the sheets at different frequencies.

Delaminated Samples	Experimental results using LCR meter		
	Change in Capacitance (pf)		
Change in area (mm^2)	1Khz	100Khz	200Khz
1. 50x55	5.1637	1.8655	7.0518
2. 50x105	9.3876	2.3799	7.7727
3. 50x155	18.428	8.8904	12.677

Figure 4.16 shows the simulated and experimental results obtained in terms of capacitance with the variation in the size of delamination in the specimen. Here both simulated and experimental results prove the increasing trend of capacitance.

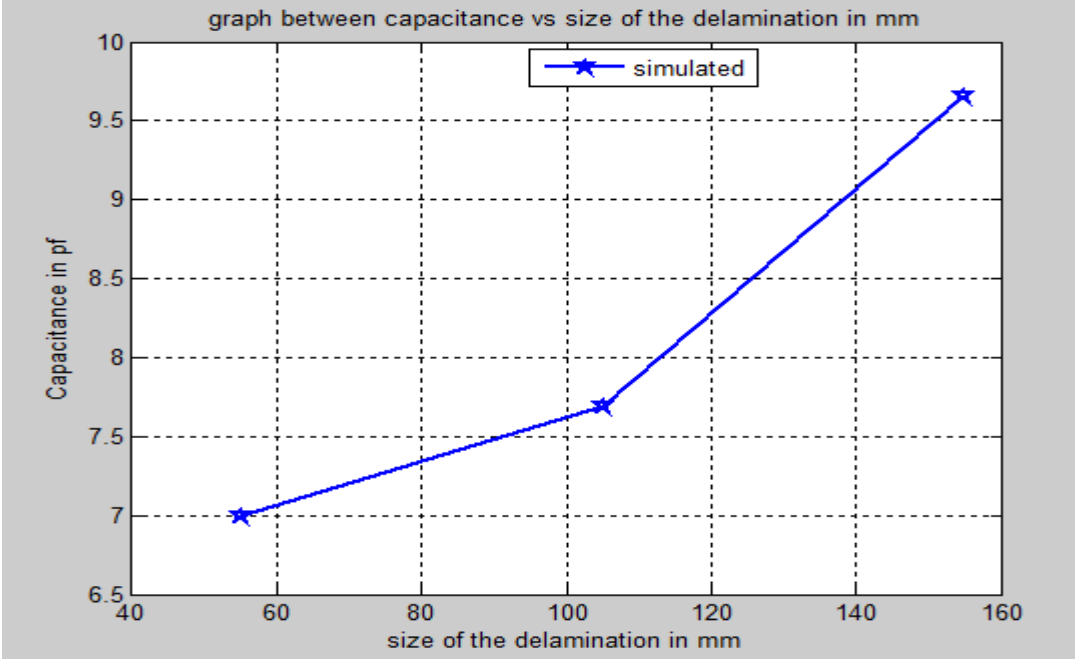

(a)

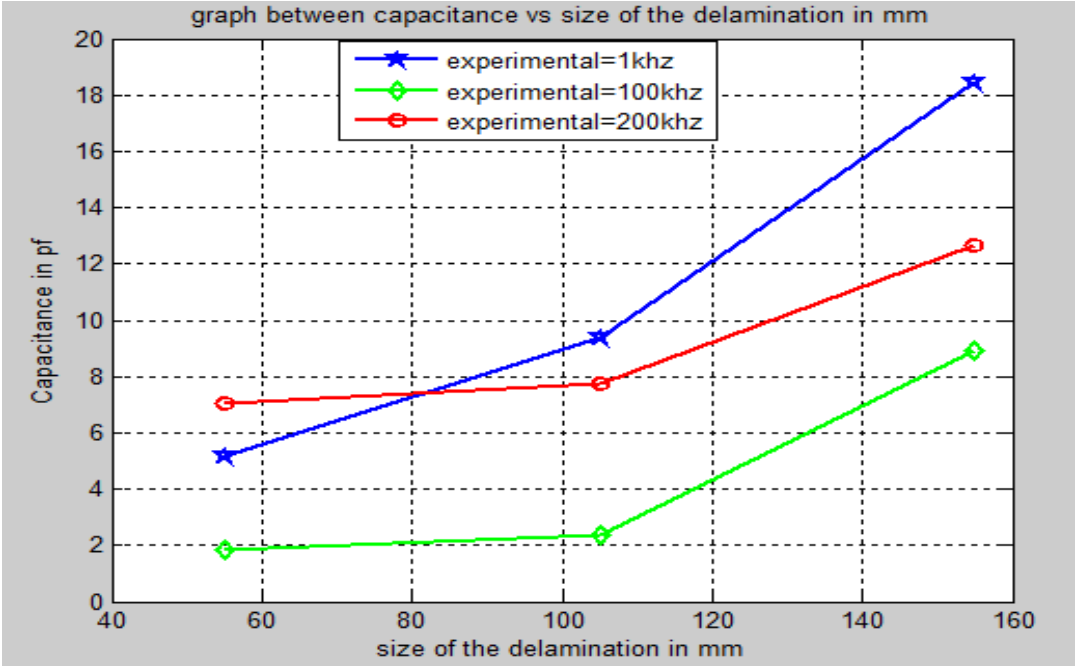

(b)

Figure 4.16 Variation of Capacitance versus Size of delamination (a) simulated results (b) experimental results

Here figure 4.17 shows the comparison between the experimental and simulated results in terms of capacitance of CPS with the variation in the dimension of the delamination. We observed from the experimental results that with the increase in the dimension of the delamination, capacitance increases sharply as compared to the simulated results.

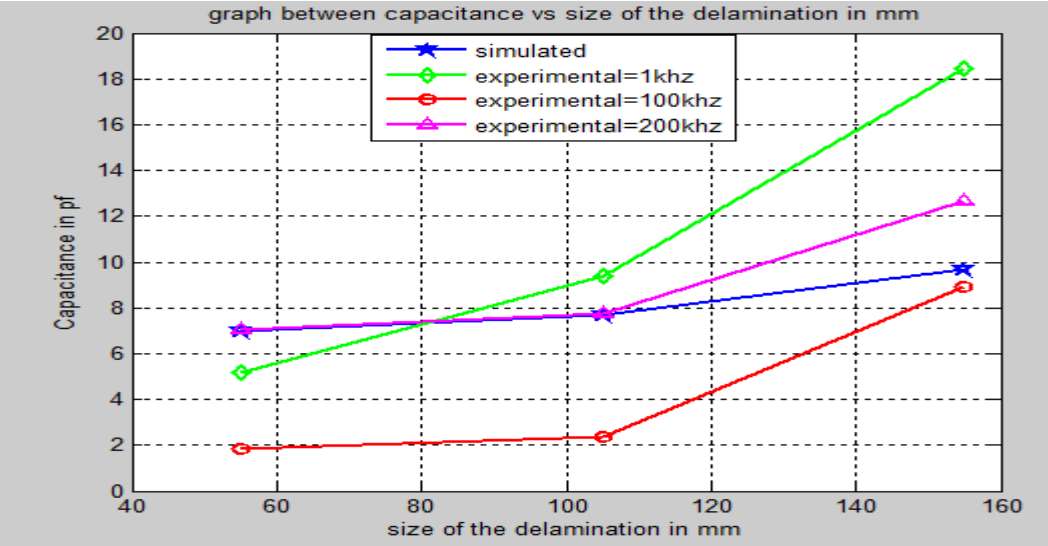

Figure 4.17 Comparison between simulated and experimental results with variation of capacitance versus size of delamination

4.10 Effect of Defects in GFRP wrapped Concrete over Capacitance

4.10.1 Simulated Results

It was observed that with the increase in the width of the void from 2-10 mm in concrete, assigned dielectric permittivity of air, capacitance decreases as shown in figure 4.18

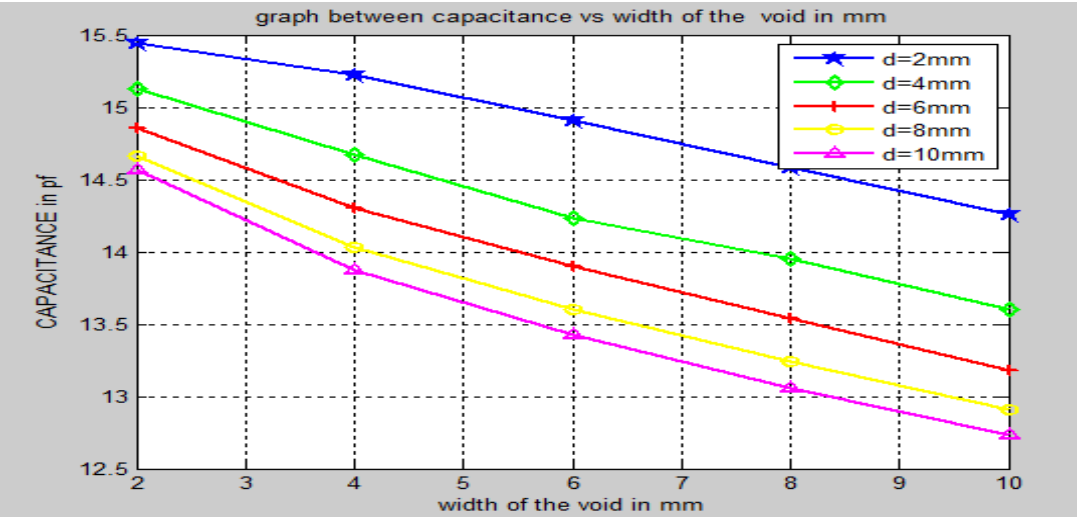

Figure 4.18 Variation of capacitance with width of the void (ε_r =1)

It was observed that with the increase in the width of the void from 2-10 mm in concrete, assigned dielectric permittivity of water, capacitance increases as shown in figure 4.19

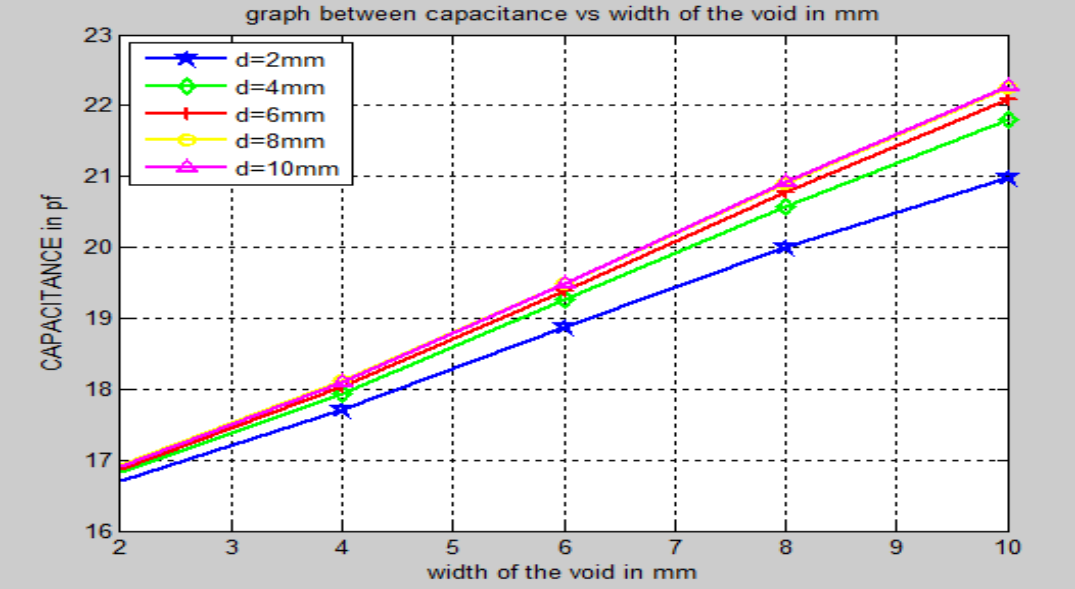

Figure 4.19 Variation of capacitance with width of the void (ε_r =81)

4.10.2 Experimental Results

It was observed that with the increase in the width of the void from 60-100 mm at the concrete-GFRP interface, assigned dielectric permittivity of air,capacitance decreases.

Table 4.4 Comparison between Simulated, Experimental and theoretical results with the presence of defects in GFRP wrapped concrete.

GFRP Wrapped Concrete	Simulated values (ε_r=1)	Experimental values (ε_r=1)	Theoretical value
Void Size (mm^2)	Capacitance (pf)	Capacitance (pf)	Capacitance (pf)
1. No Void	14.1340	28.589	5.099
2. 50x60	10.3135	22.140	-
3. 50x100	6.3068	11.345	-

Figure 4.20 shows the comparison between the experimental and simulated results in terms of capacitance of CPS with the variation in the size of the gap at the concrete-GFRP surface.

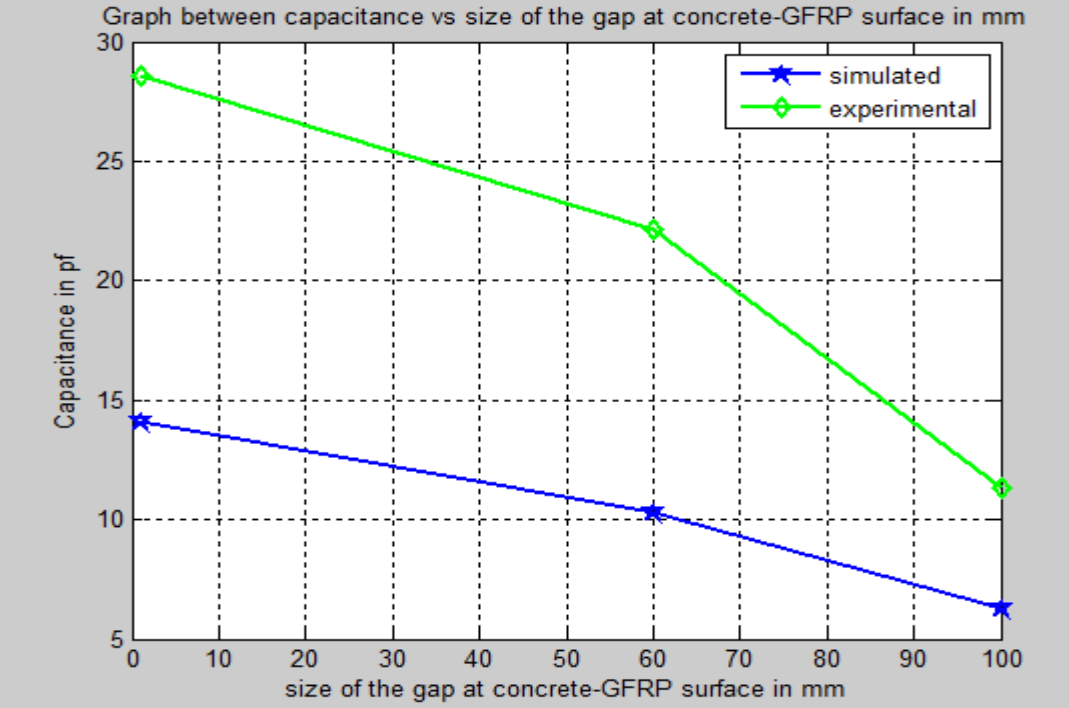

Figure 4.20 Variation of capacitance versus size of the gap at the concrete-GFRP surface.

Chapter 5

Defect detection in Concrete using Microstrip patch antenna

In this chapter results at high frequency were discussed. The presence of defects in the concrete was measured by finding the changing in the reflection coefficient (return loss) and resonant frequency of the micro strip patch antenna at high frequency. Before going to discuss the results, introduction of micro-strip patch antenna is given in section 5.1.

5.1 Introduction of Micro-strip patch antenna

A Micro-strip patch antenna consists of a radiating patch on one side of a dielectric substrate which has a ground plane on the other side as shown in figure 6.1.The patch is generally made of conducting material such as copper or gold and can take any possible shape. The radiating patch and the feed lines are usually photo etched on the dielectric substrate.

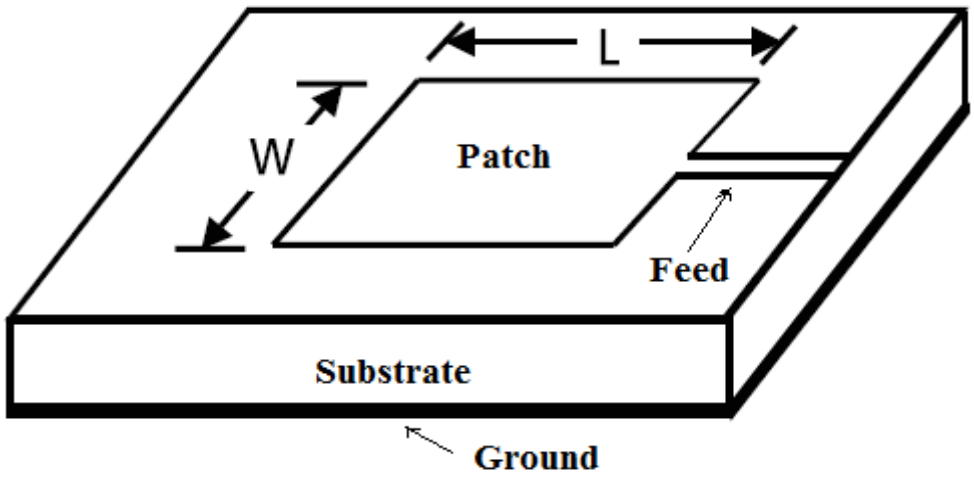

Figure 5.1 Basic Structure of an Antenna[32]

In order to simplify analysis and performance prediction, the patch is generally square, rectangular, circular, triangular and elliptical or some other common shapes. For a rectangular patch, the length L of the patch is usually $0.3333\lambda_0 < L < 0.5\lambda_0$, where λ_0 is the free-space wavelength. The patch is selected to be very thin such that $t << \lambda_0$ (where t is the patch thickness). The height h of the dielectric substrate is

usually $0.003\,\lambda_0 \leq h \leq 0.05\,\lambda_0$. The dielectric constant of the substrate (ε_r) is typically in the range $2.2 \leq \varepsilon_r \leq 12$.

5.1.1 Mathematical formulas to design an antenna

The following formulas are used to design an antenna which is given below:-

$$L_{eff} = L + 2\Delta L \qquad (5.1)$$

$$\varepsilon_{reff} = \frac{\varepsilon_r+1}{2} + \frac{\varepsilon_r-1}{2}\left[1 + 12\frac{h}{W}\right]^{-\frac{1}{2}} \qquad (5.2)$$

$$\frac{\Delta L}{h} = 0.412\frac{(\varepsilon_{reff} + 0.3)(\frac{W}{h} + 0.264)}{(\varepsilon_{reff} - 0.258)(\frac{W}{h} + 0.8)} \qquad (5.3)$$

$$L = \frac{1}{2f_r\sqrt{\varepsilon_{reff}}\sqrt{\mu_0\varepsilon_0}} - 2\Delta L \qquad (5.4)$$

$$W = \frac{1}{2f_r\sqrt{\mu_0\varepsilon_0}}\sqrt{\frac{2}{\varepsilon_r + 1}} \qquad (5.5)$$

Where ε_r= substrate permittivity

5.1.2 Structure of Proposed antenna

In figure 5.2, the proposed antenna is shown, and the antenna from the patch side is sited on the concrete specimen. By radiating patch, analyze the reflection coefficient and resonant frequency. According to the theoretical values, with given length and width of patch 40mm and 50mm respectively, calculated from the above formulas our antenna should be resonating at **2.2 GHz** but during simulation it is resonating at **1.87 GHz.**

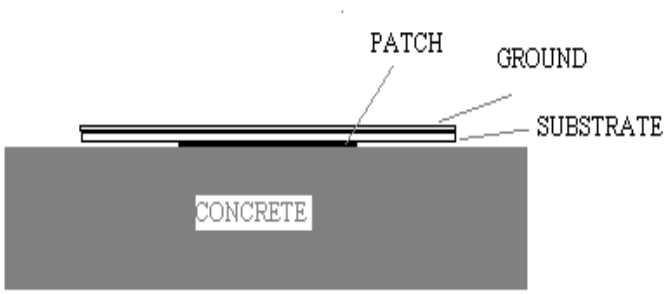

Figure 5.2 Structure of proposed antenna

In figure 5.3 different type of voids artificially created in CST 9.0 Microwave studio software is shown.

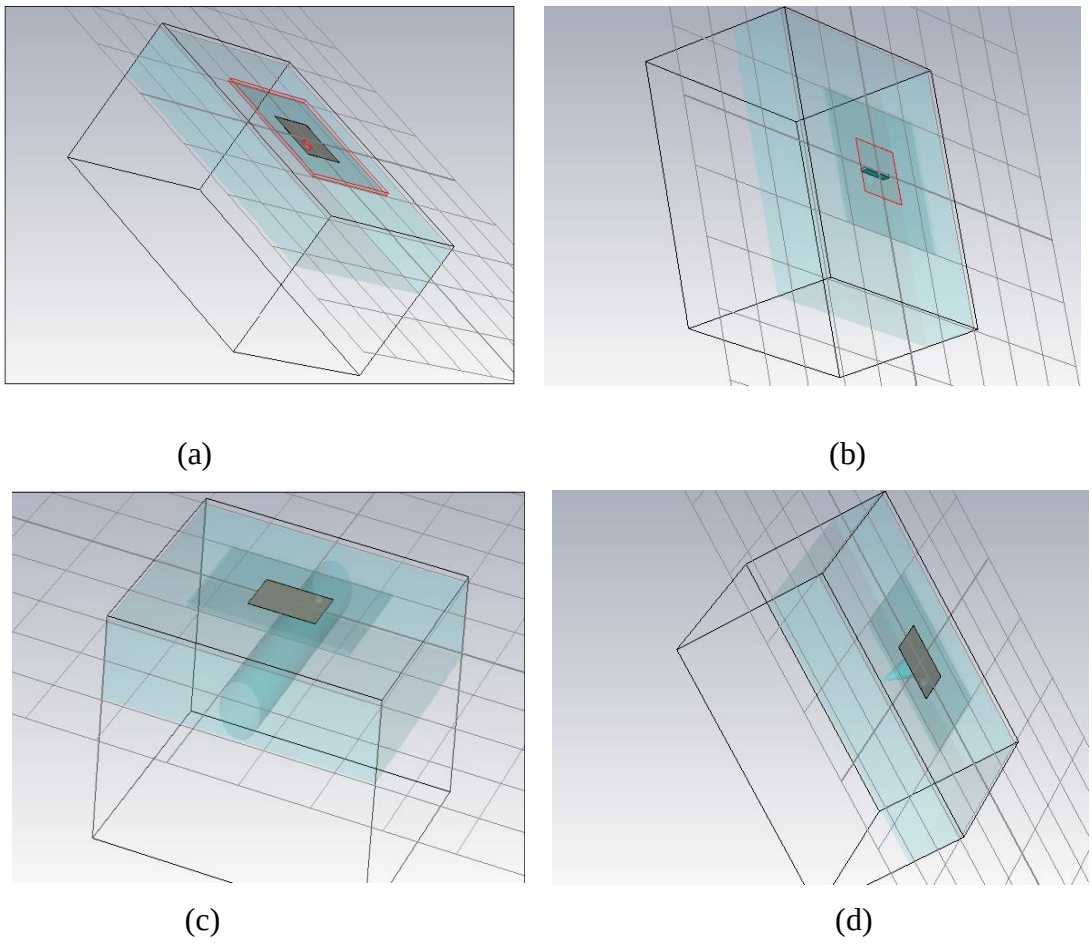

Figure 5.3 Antenna with different type of voids in CST (a) without any void (b) with rectangular void (c) with steel rebar (d) with cone void

5.2 Effect of Defects over Reflection coefficient and Resonant Frequency shift

In this thesis work is done at low frequency. We can use different software's to work at high frequency. We can also detect the defects in the concrete by applying the high frequency at the input of copper strips in the GHz range and detect the change in the reflection coefficient with the help of CST Microwave studio. But here the coaxial feed micro-strip patch antenna is used for the simulation purpose. CST MICROWAVE STUDIO® is a fully featured software package for electromagnetic analysis and design in the high frequency range. It simplifies the process of inputting the structure by providing a powerful solid modelling front-end which is based on the

ACIS modelling kernel. Strong graphic feedback simplifies the definition of your device even further. After the component has been modelled, a fully automatic meshing procedure (based on an expert system) is applied before the simulation engine is started. Using this software we have studied the return loss and change in the resonant frequency due to the presence of the defects. Here we varied the depth, d of the void in the concrete. We can see the change in the return loss in figure's 5.4 to 5.10

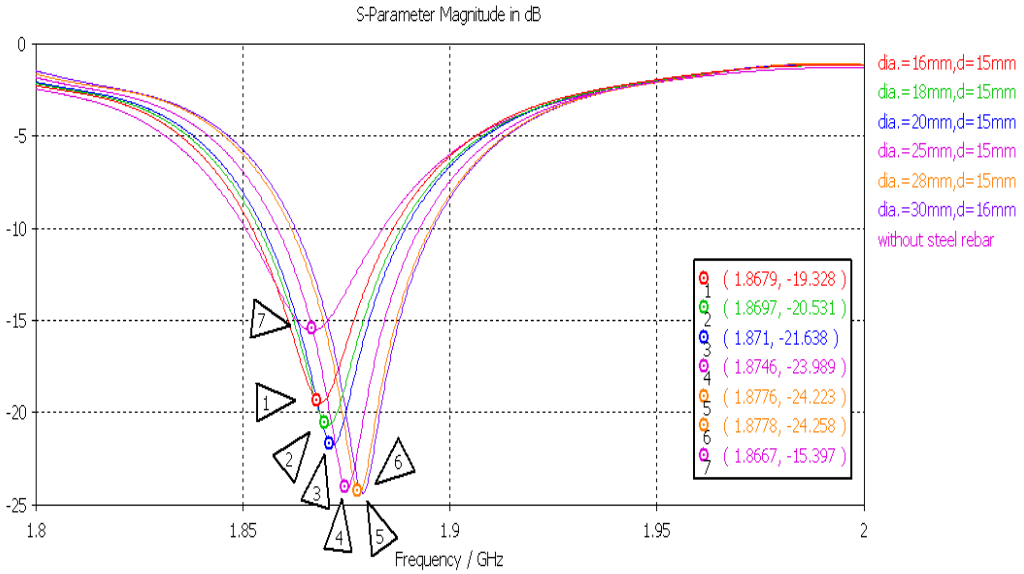

Figure 5.4 Return loss with Steel rebar (ε_r=3.1) at d=15 mm

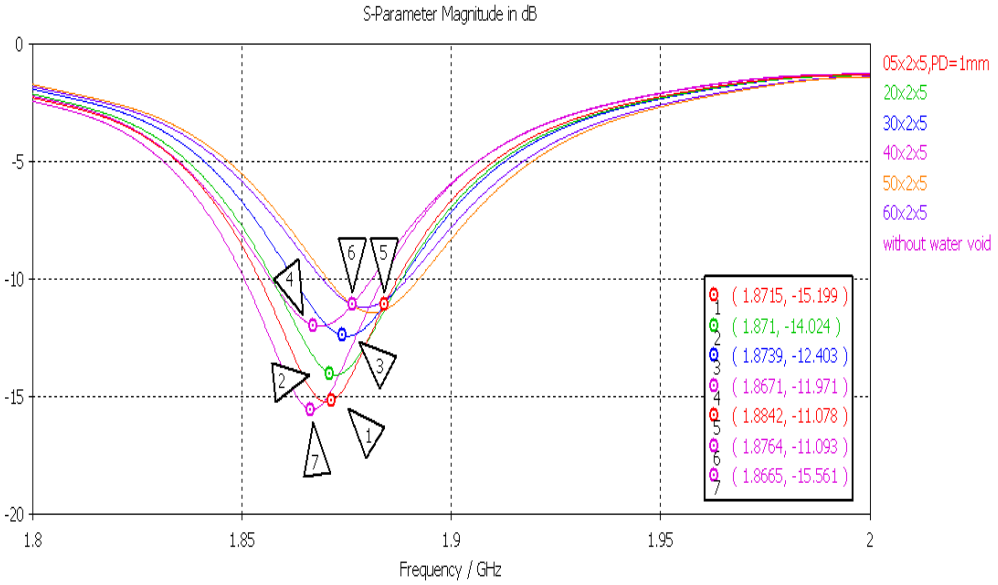

Figure 5.5 Return loss with rectangular defect (ε_r=81) at d=5mm

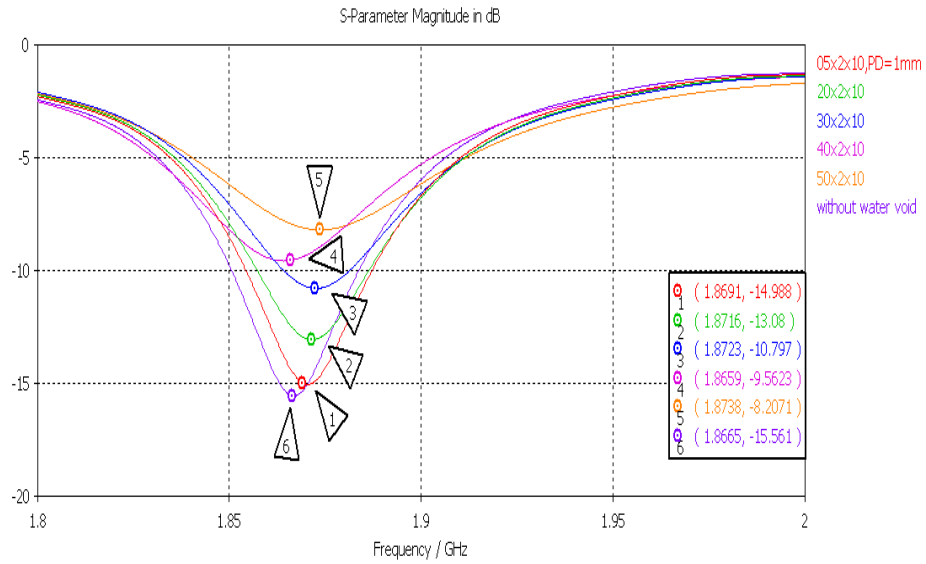

Figure 5.6 Return loss with rectangular defect (ε_r=81) at d=10mm

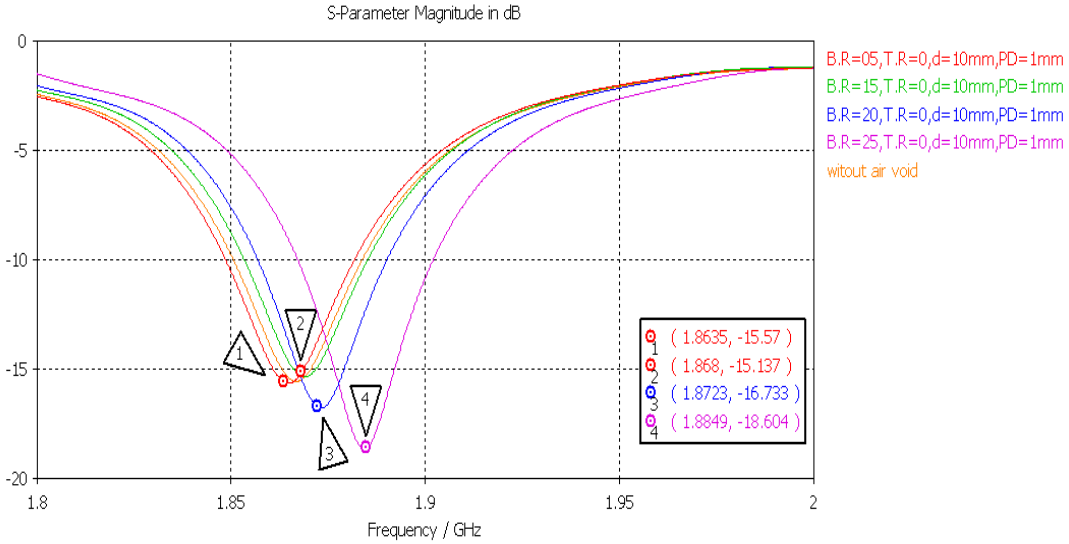

Figure 5.7 Return loss with cone defect (ε_r=1) at d=10mm

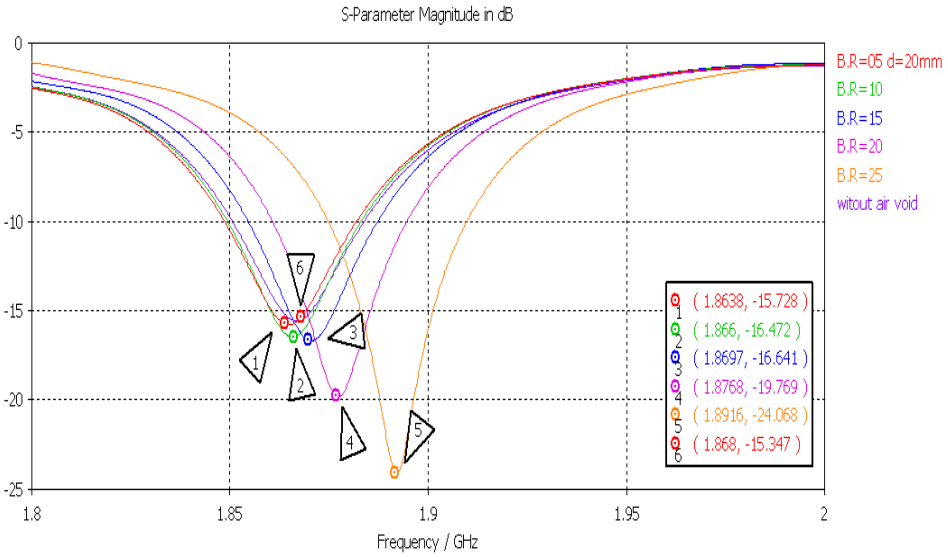

Figure 5.8 Return loss with cone defect (ε_r=1) at d=20mm

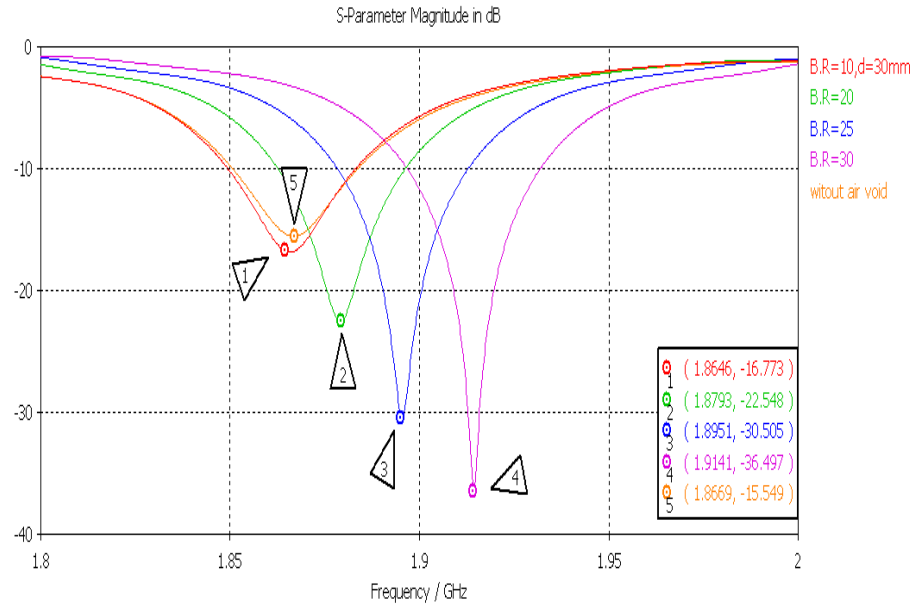

Figure 5.9 Return loss with cone defect (ε_r=1) at d=30mm

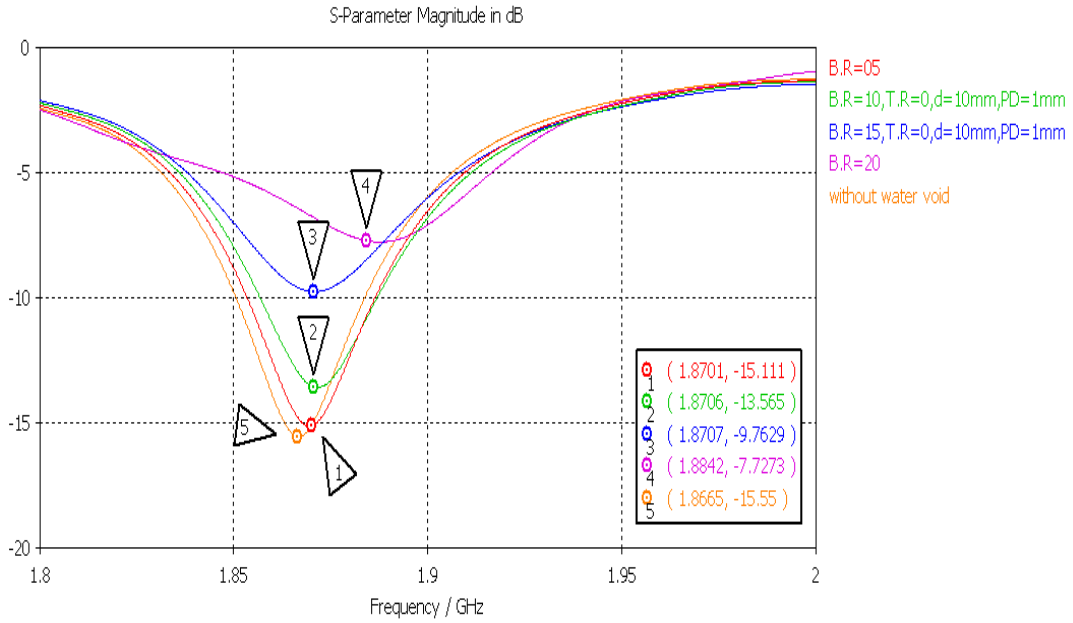

Figure 5.10 Return loss with cone defect (ε_r=81) at d=10mm

Figure 5.11 and 5.12 shows the graphical variation in terms of resonant frequency of the micro strip patch antenna with the change in the diameter of steel rebar and bottom radius of cone at depth, d=5mm and d=10,20,30mm respectively.

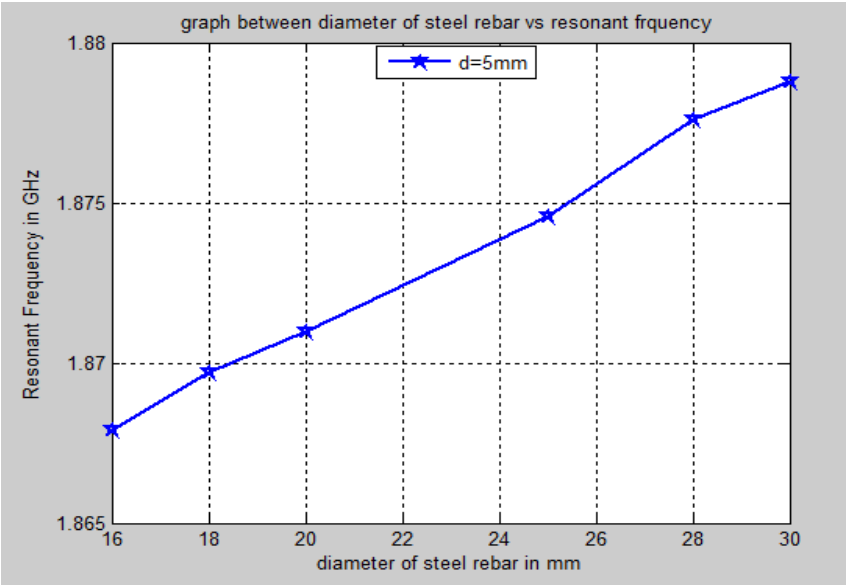

Figure 5.11 Diameter of steel rebar versus resonant frequency at depth =5mm

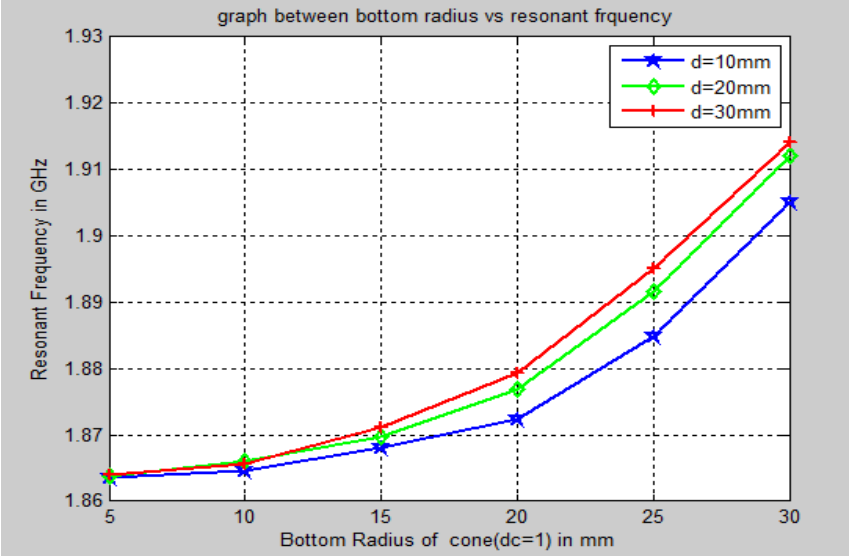

Figure 5.12 Bottom radius of cone versus resonant frequency at different depths

5.3 Effect of Moisture absorption over Resonant Frequency shift

The effect of moisture ingress is analyzed by changing the dielectric constant of the substrate with the given relation shown by eqn. no. **5.6** [10]

$$\varepsilon_r=\varepsilon_{fr4}+M(\varepsilon_w-\varepsilon_{fr4}) \quad (5.6)$$

Here M is the moisture ingress in % and ε_{fr4} and ε_w is the relative dielectric constant of FR4 (~4.4) substrate and water (~80) respectively.

Table 5.1 Change in resonant frequency w.r.t. moisture absorption ratio (%)

S. No	Dielectric constant	Resonant frequency (GHz)		Return loss (dB)		Moisture absorption
		1st peak	2nd peak	1st peak	2nd peak	%
1	4.4	5.5	6.0	-19	-19	0.0
2	4.5512	5.4	5.9	-19.5	-14.5	0.2
3	4.7024	5.3	5.8	-19	-16.5	0.4
4	4.8536	4.95	5.7	-19.5	-18	0.6
5	5.0048	4.8	5.6	-20	-18	0.8
6	5.156	4.65	5.5	-20	-17	1.0
7	5.3072	4.6	5.45	-20	-16	1.2
8	5.4584	4.55	5.4	-20.5	-14	1.4
9	5.6096	4.52	5.35	-22	-12.5	1.6
10	5.7608	4.51	5.25	-22.15	-15	1.8
11	5.912	4.45	5.2	-22	-18	2.0

Table 5.1 shows that as the moisture ingress (%) increases, the dielectric constant also increases and resonant frequency decreases. In Figure 5.13 to 5.23 we can see the variation in the resonant frequency that with the increase in the moisture ingress level, resonant frequency of micro-strip patch antenna decreases, with the increase in the dielectric permittivity value using equation no.5.6.

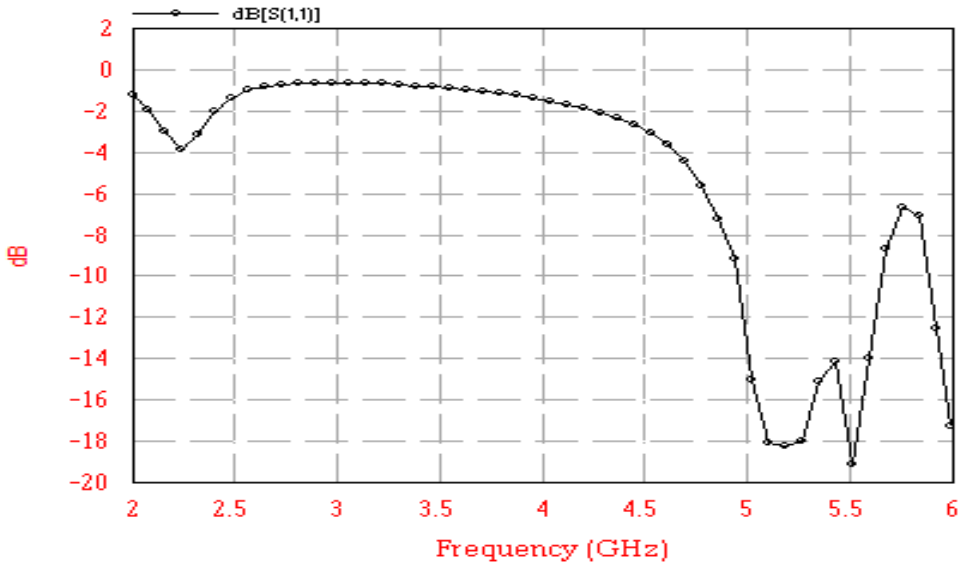

Figure 5.13 Resonant frequency and Return loss at $\varepsilon_{r=}$4.4, M=0%

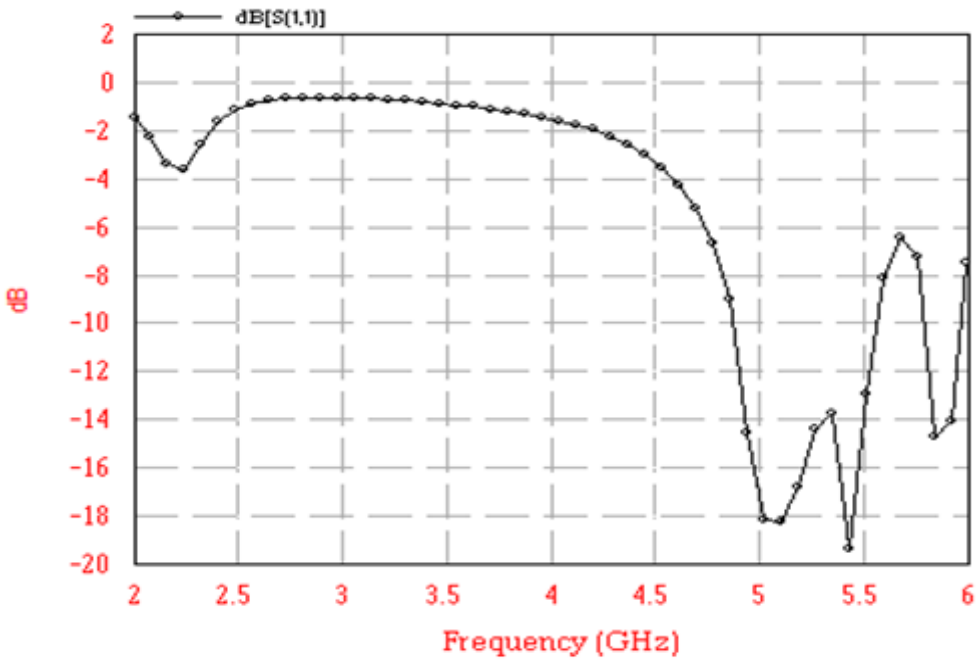

Figure 5.14 Resonant frequency and Return loss at $\varepsilon_{r=}$4.5512, M=0.2%

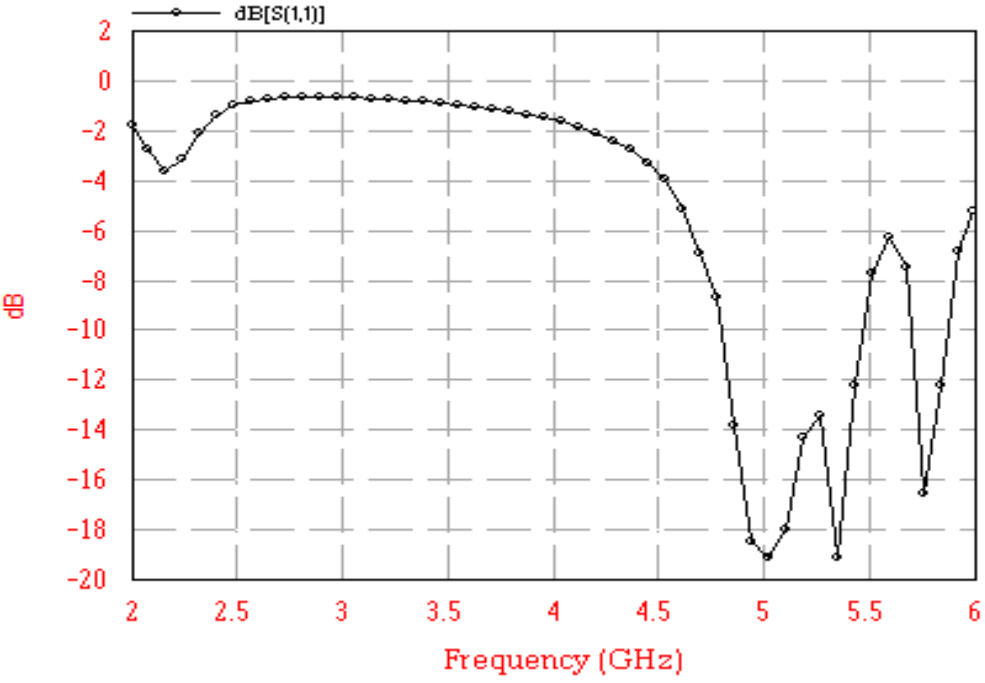

Figure 5.15 Resonant frequency and Return loss at $\varepsilon_{r=}$4.7024, M=0.4%

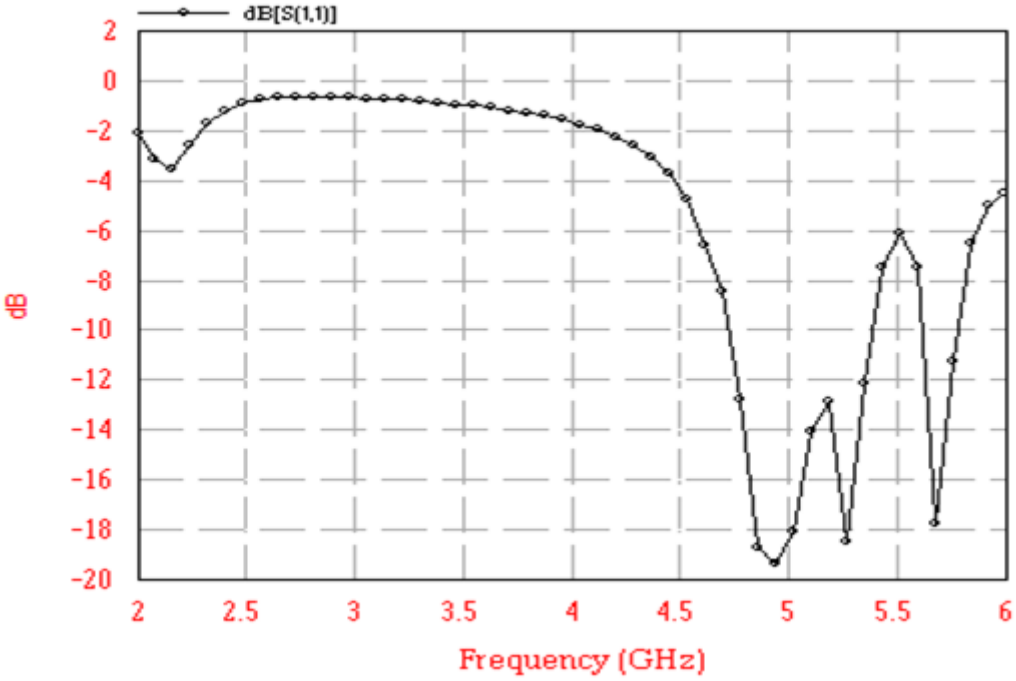

Figure 5.16 Resonant frequency and Return loss at $\varepsilon_{r=}$4.8536, M=0.6%

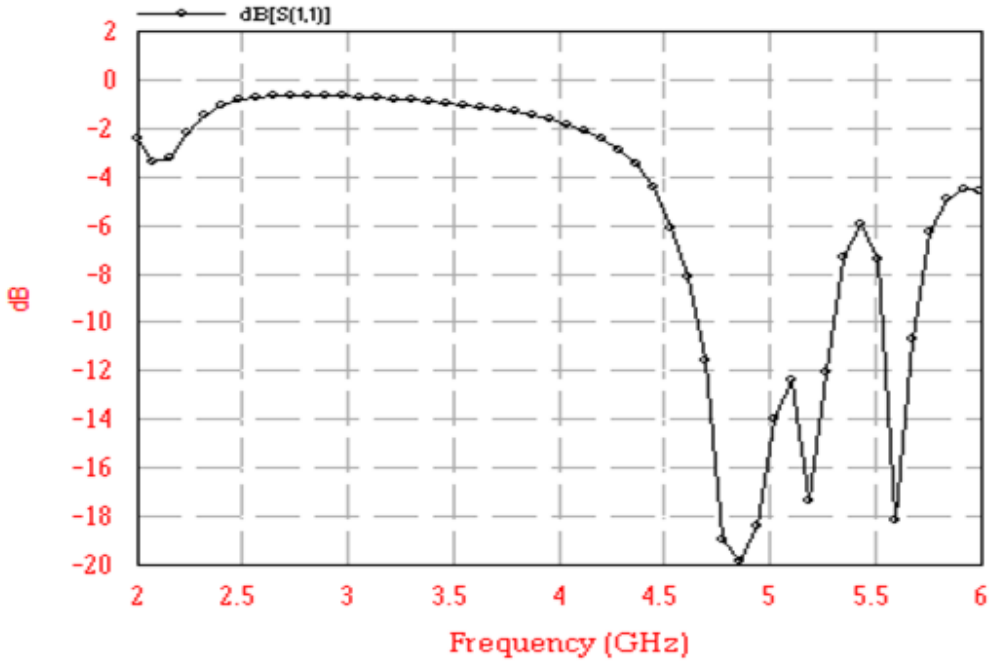

Figure 5.17 Resonant frequency and Return loss at $\varepsilon_{r=}$5.004, M=0.8%

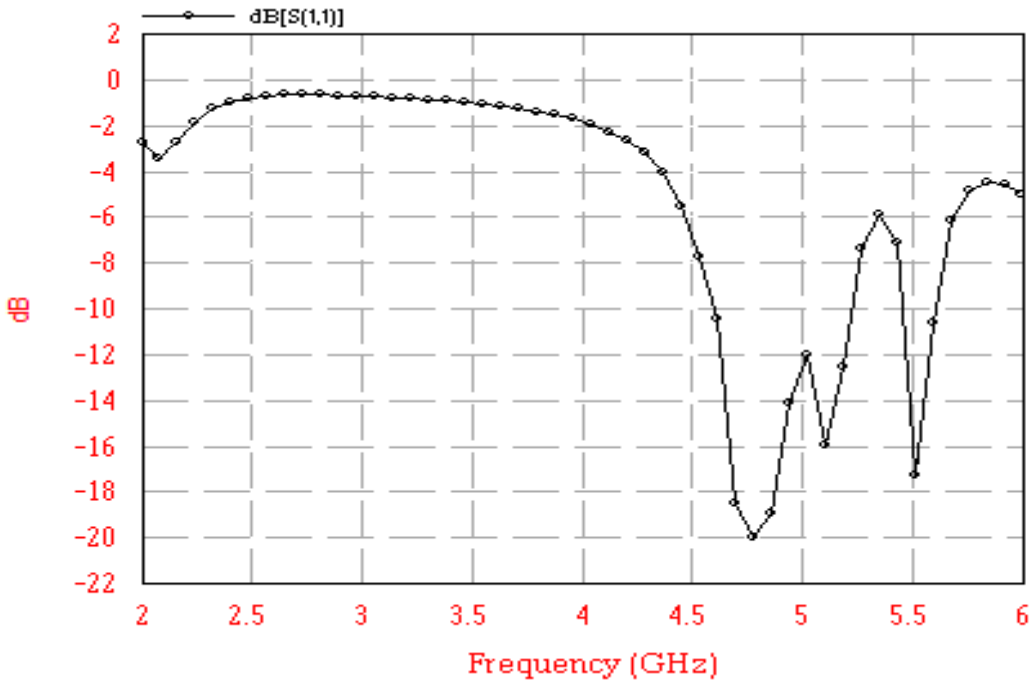

Figure 5.18 Resonant frequency and Return loss at $\varepsilon_{r=}$5.156, M=1%

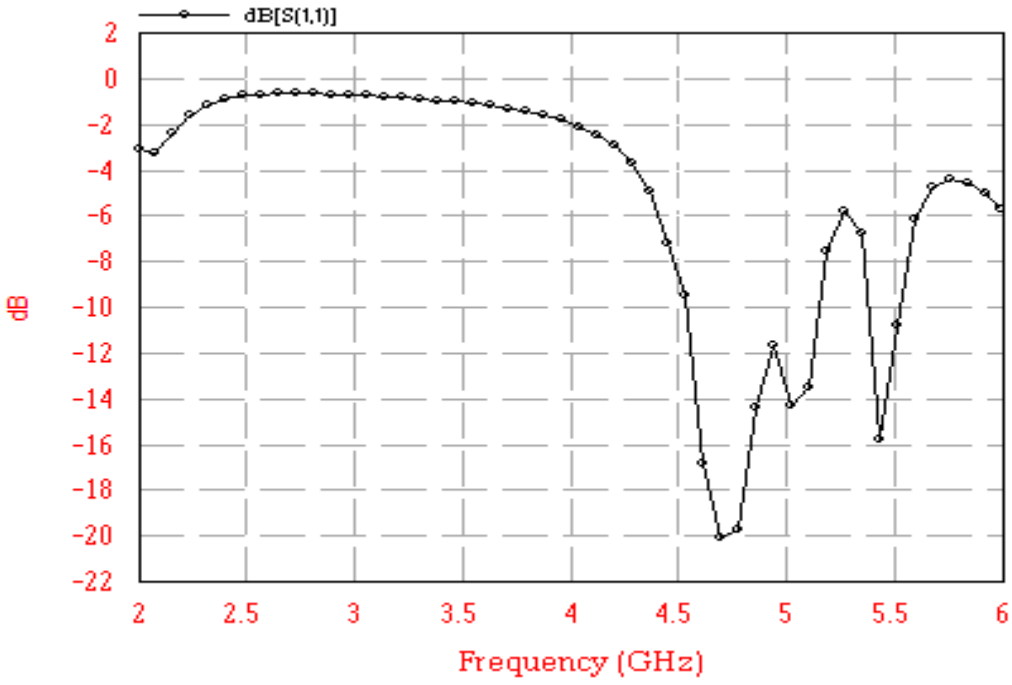

Figure 5.19 Resonant frequency and Return loss at $\varepsilon_{r=}$5.3072, M=1.2%

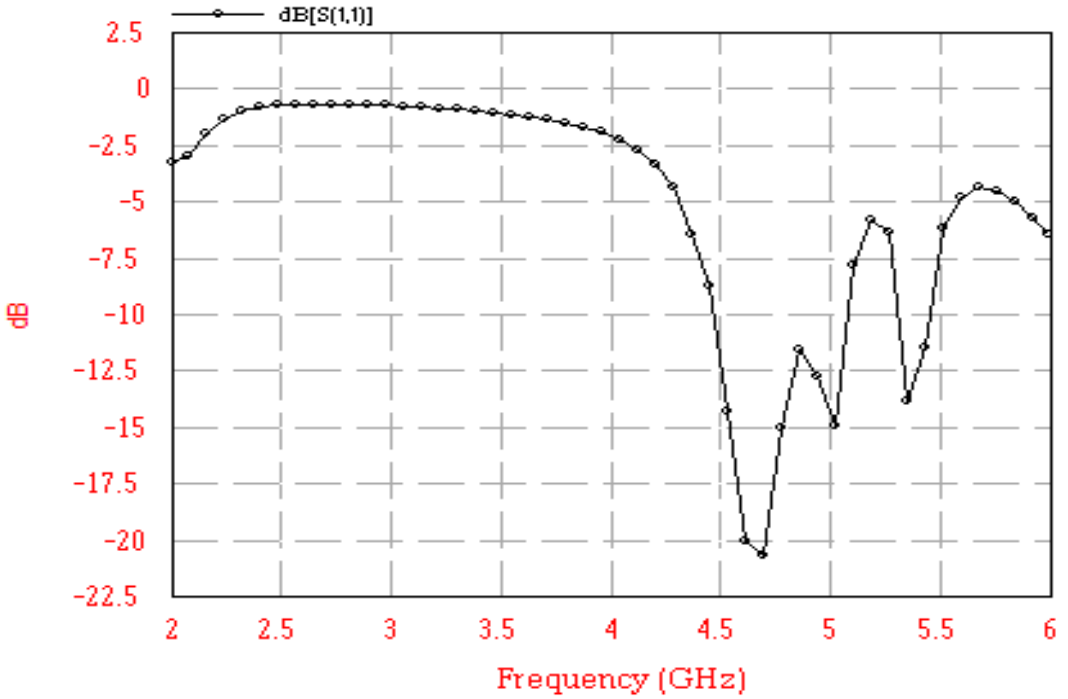

Figure 5.20 Resonant frequency and Return loss at $\varepsilon_{r=}$5.4584, M=1.4%

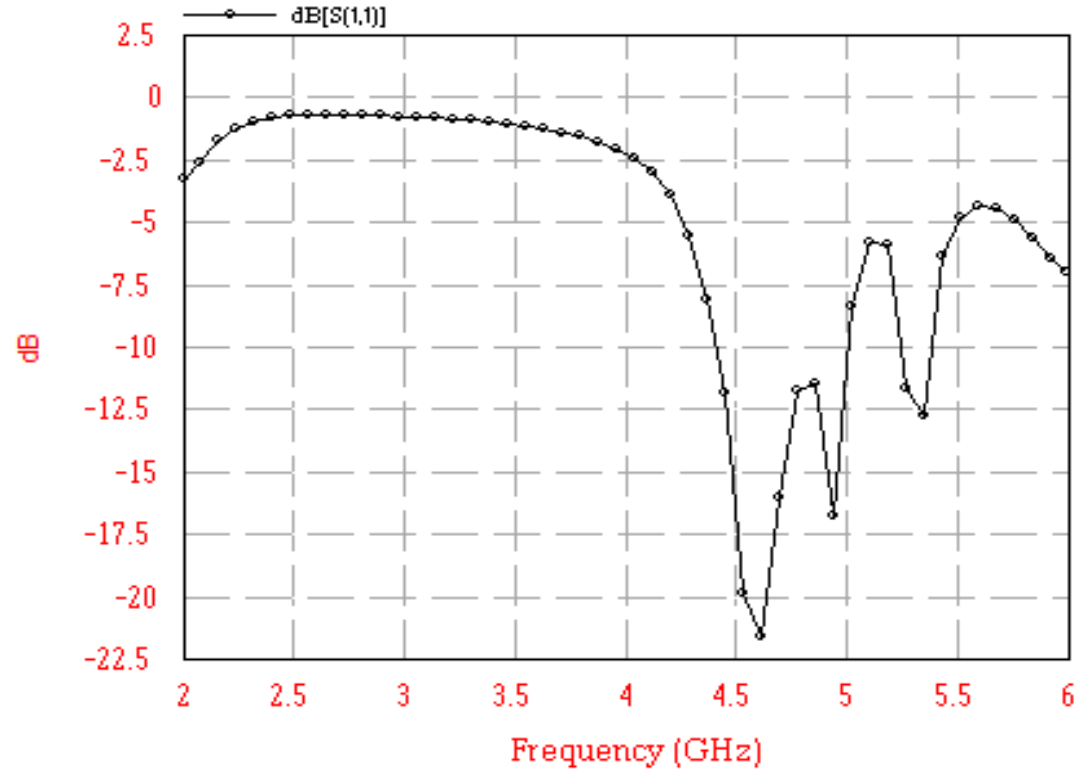

Figure 5.21 Resonant frequency and Return loss at $\varepsilon_{r=}$5.6096, M=1.6%

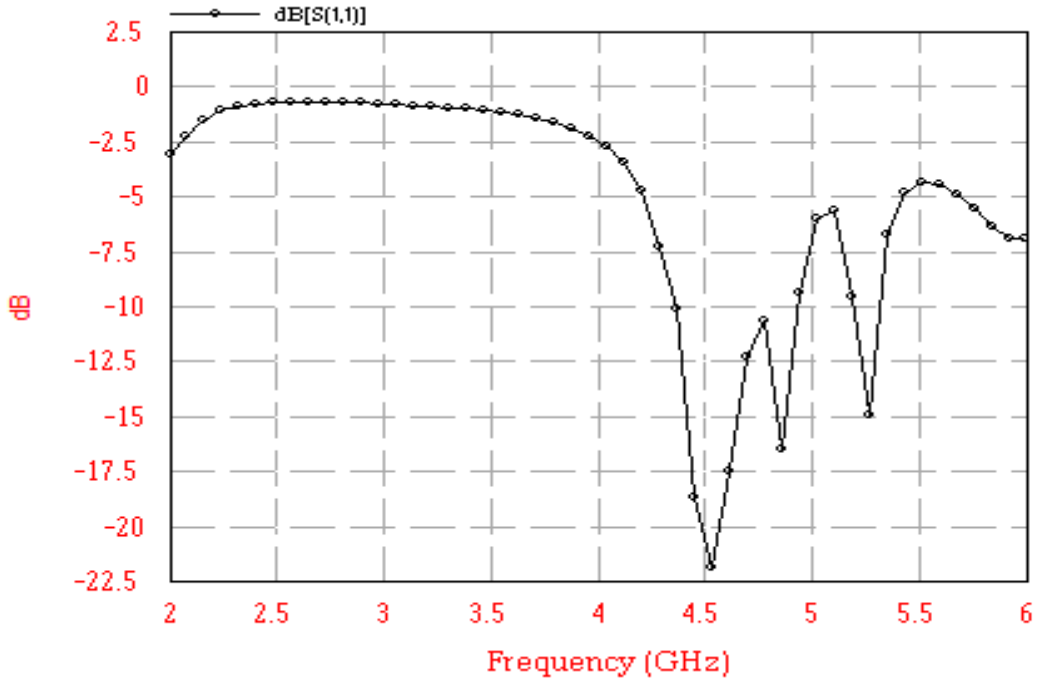

Figure 5.22 Resonant frequency and Return loss at $\varepsilon_{r=}$5.7608, M=1.8%

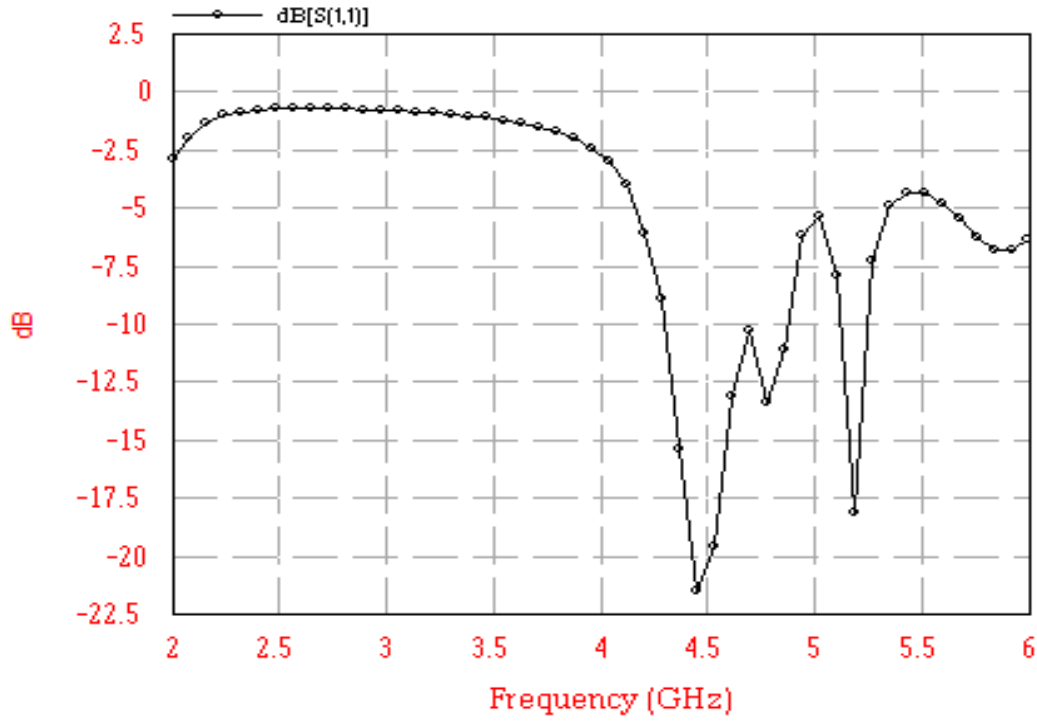

Figure 5.23 Resonant frequency and Return loss at $\varepsilon_{r=}$5.912, M=2%

Figure 5.24 shows the graphical variation in terms of resonant frequency with the variation in the moisture absorption. Here relative variation in between resonant frequencies is also shown.

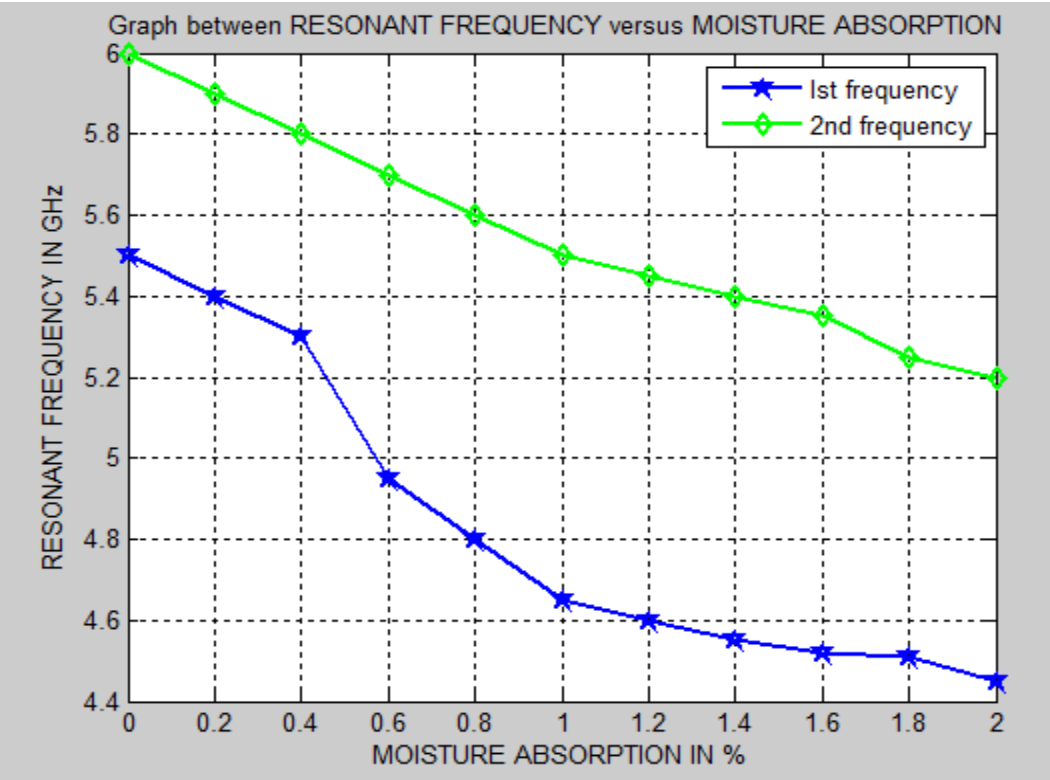

Figure 5.24 Resonant Frequency versus Moisture absorption (%)

Chapter 6

Conclusion and Future Scope

6.1 Conclusion

FRPs are invariably exposed to varying environments, both in storage and in operation. Since water and air is omnipresent in the environment, concern has arisen about the nature of the interaction of environment with materials like GFRP, CFRP and Concrete and their effects on the material properties of FRP's. Water and air could diffuse to the fiber-matrix interface, and this can cause weakening of the interface. The matrix material could be plasticized or degraded due to absorption of water and air resulting in deteriorated mechanical properties. It is therefore essential to monitor the amount of water and air into the FRP by NDT.

In this thesis, the defect detection in GFRP and Concrete is found through modelling, experimentally. The defects are found in terms of capacitance of coplanar strip line. A new method of finding the defect in terms of frequency shift and return loss using micro-strip patch antenna at high frequency is also discussed here. The main conclusions drawn are given as under:

6.1.1 At low frequency using CPS

- It has been observed that with the increase in the width of the void from 2-10 mm in concrete, assigned dielectric permittivity of air, capacitance decreases and if assigned dielectric permittivity of water to the void then, capacitance increases.
- And with the increase in the length of delamination sheet, capacitance increases.

6.1.2 At high frequency using MSPA

- With the increase in moisture ingress on the substrate of the micro-strip patch antenna, dielectric permittivity increases and resonant frequency decreases.
- Return loss decreases and resonant frequency increases with the increase in the diameter of the steel rebar in concrete.
- Return loss increases, with the increase in length of the rectangular water void in concrete.

- Return loss decreases and resonant frequency increases, with the increase in the bottom radius of the air cone void in concrete.
- Return loss increases, with the increase in the bottom radius of the water cone void in concrete.

6.2 Future Scope

In this thesis, the effect of defects and effect of delamination on the capacitance of CPS at low frequency and effect of defects on the resonant frequency and return loss at high frequency is studied. In this thesis symmetrical and asymmetrical defects were studied on the GFRP wrapped concrete structures. There can be a defect in the fiber-matrix bond. So we can also measure the capacitance by creating the defects artificially in fiber-matrix bond. There are so many issues in the areas of structural health monitoring (SHM) which need to be solved. But a new technique based on Fibre Optic Sensor we can use it to find the air gap and crack as well as for structural health monitoring in future. Further one can design an electronic instrument which can correlate the value of capacitance with the void, crack and delamination.

REFERENCES

[1] http://www.ndt-ed.org/GeneralResources/IntroToNDT/GenIntroNDT.htm,last accessed on June 15, 2011.

[2] http://www.netcomposites.com/education.asp, last accessed on June 15, 2011.

[3] A.D. Jaffery, "Concrete filled Glass Reinforced Shells under Concentric Compression", Thesis for Master of Aied Science, University of Tornado, 2001

[4] D.V. Elinde, L. Zhao, F. Seible, "Use of FRP in Civil Structural Applications" Construction and Building Materials, Vol.17, No. 6-7, pp. 389-403, 2003.

[5] http://www.quakewrap.com/technical-papers-on-Fiber-Reinforced-Polymer.php, last accessed on June 15, 2011.

[6] http://www.autospeed.com/composites.html, last accessed on June 18, 2011.

[7] P. Thomas, K. Dwarakanath, P. Sampathkumaran, S. Seetharamu and Kishore, "Influence of moisture absorption on electrical characteristics of glass-epoxy polymer composite system," International Symposium on Electrical Insulating Materials, Vol. 3, pp. 612-615, 2005

[8] Dakhakhni et al., "Damage Detection of FRP-Strengthened Concrete Structure Using Capacitance Measurements", Journal of Composites for Construction, Vol.13, No.6, 2009.

[9] X. Yin, G.G. Diamond, D.A. Hutchins, "Further investigations into capacitive Imaging" for NDE, Journal on British Institute Non-Destructive Testing, Vol. 51, No. 9, pp. 484–490, 2009.

[10] G. D. Davis, M. J. Rich and L. T. Rizal, "Monitoring Moisture Uptake and De lamination in CFRP-Reinforced Concrete Structures with Electrochemical Impedance Sensors", Journal of Non-destructive Evaluation, Vol. 23,No. 1, pp. 1-9, 2004.

[11] Y. Shimamura, T. Urabe, A. Todoroki and H. Kobayashi, "Measurement of Moisture Absorption Ratio of FRP using Micro Polymer Sensor", Journal on Key Engineering Materials, Vol. 270-273, pp. 1957-1964, 2004.

[12] M. Bogosanovich, “Micro-strip Patch Sensor for Measurement of the Permittivity of Homogeneous Dielectric Materials”, IEEE Transactions on Instrumentation and Measurement, Vol. 49, No. 5, 2000.

[13] A. Cataldo, G. Monti, G. Cannazza, E. De Benedetto, L. Tarricone, M. Cipressa, “Non-Invasive Approach for Moisture Measurements through Patch Antennas”, IEEE International Conference on Instrumentation and Measurement Technology, pp. 1012-1015, 2008.

[14] R. Wakodkar, B. Gupta, S. Chakraborty, “Variation of Resonant Frequency of a Rectangular Microstrip Patch Antenna Due to Accumulation of Water over its Surface” International Conference on Applications of Electromagnetism and Student Innovation Competition Awards, pp. 239-243, 2010.

[15] K. M. Z. Shams, M. Ali, and A. M. Miah, “Characteristics of an Embedded Microstrip Patch Antenna for Wireless Infrastructure Health Monitoring”, IEEE International Symposium on Antennas and Propagation Society, pp. 3643-3646, 2006.

[16] M. Q. Feng, C. Liu, X. He, and M. Shinozuka, “Electromagnetic Image Reconstruction for Damage Detection”, Accepted for publication in Journal of Engineering Mechanics, ASCE, 2000.

[17] Muhammad Hassan Bin Afzal, Shahid Kabir, “Fiber Optic Sensor-based Concrete Structural Health Monitoring”, IEEE, 2011.

[18] Eli Chen, Chou S. Y., “Characteristics of coplanar transmission lines on Multilayer Substrates: Modelling and experiments”, IEEE Transactions on Microwave Theory and Techniques, Vol. 45, No. 6, pp. 939-945, 1997.

[19] S.Georgian and H.Berg, “Line Capacitance and Impedance of Coplanar Strip Waveguides on Substrates with Multiple Dielectric Layers,” 31st European Conference on Microwave, pp.1-4, 2001. [7] E. Carlson and S. Georgian., “Conformal mapping of the field and charge distributions in multilayered substrate CPWs”, IEEE Transactions on Microwave Theory and Techniques, Vol.47, No. 8, pp.1544-1552, 1999.

[20] S. Georgian, H. Berg, H. Jacobs son, and T. Le win, "Application notes – basic parameters of coplanar-strip waveguides on multilayer dielectric/semiconductor substrates, Part 1: high permittivity supersaturates," IEEE Transaction on Microwave Magazine, Vol. 4, pp. 60-70, 2003.

[21] K.C. Gupta, R. Garg, I. Bahl, and P. Bhartia, Microstrip Lines and Slot line. Norwood, MA: Artech House, 1996.

[22] K. Heindl, T. Blecha, V. Skocil and J. Braun, "Mathematic model of coplanar strip", pp. 209-212, SPI 2006.

[23] R.N. Simon, Coplanar Waveguide Circuits, Components and Systems. New York: Wiley, 2001.

[24] http://www.moldedfiberglass.com/library/da/Composite_Tech&Tech.pdf, last accessed on June 22, 2011.

[25] A. Sharma, R. Chhibber and A. Mukherjee, "Environmental Degradation of Glass Fibre Reinforced Polymer Composites" Degree: M.E. 2009, Thapar University, Patiala. URL:http://hdl.handle.net/10266/1045

[26] American Institute of Aeronautics and Astronautics- Effects of Glass Fabric and Laminate Construction on the Fatigue of Resin Infused Blade Materials by Daniel D. Samborsky and John F. Mandell.

[27] A. P Prudnikov, Yu. A Brychkov, Integrals and Series's, Gordon and Breach, 1986.

[28] J.G. Teng, J.F. Chen, S.T. Smith & L. Lam, FRP strengthened RC structures, J. Wiley and sons, UK, 2002.

[29] K.C.Y. Leung, "Fracture mechanics of debonding failure in FRP-strengthened concrete beams", In Li et al. (ed.), Proc. FraMCoS, Vail USA, Vol. 1, pp.41-52, 2004.

[30] U. Galietti, V. Luprano, S. Nenna, L. Spagnolo, A. Tundo, "Non Destructive Defect Characterization of Concrete Structures Reinforced by means of FRP", AITA 8, September 2005, in press.

[31] K. Kesavan, K. Ravisankar, S. Parivallal, P. Sreeshylam, S. Sridhar, "Experimental Studies on Fiber Optic Sensors Embedded in Concrete Measurement", Vol.43, pp-157–163, 2010.

[32] Girish Kumar, K.P Ray, Broadband Microstrip Antennas, Artech House, Norwood, 2003.